

EXPERIMENTAL INVESTIGATION OF IMPACT OF RIGID BODIES WITH NO-SLIP CONDITION

by

DIPAK B. SHAH

ME

1986

M

SHA

EXP



DEPARTMENT OF MECHANICAL ENGINEERING

INDIAN INSTITUTE OF TECHNOLOGY KANPUR

JANUARY, 1986

EXPERIMENTAL INVESTIGATION OF IMPACT OF RIGID BODIES WITH NO-SLIP CONDITION

A Thesis Submitted
in Partial Fulfilment of the Requirements
for the Degree of

MASTER OF TECHNOLOGY

by
DIPAK B. SHAH

to the

DEPARTMENT OF MECHANICAL ENGINEERING
INDIAN INSTITUTE OF TECHNOLOGY KANPUR
JANUARY, 1986

CERTIFICATE

This is to certify that the thesis entitled, "EXPERIMENTAL INVESTIGATION OF IMPACT OF RIGID BODIES WITH NO-SLIP CONDITION" submitted by Mr. Dipak B. Shah for the award of M.Tech. degree is a record of work carried out under our supervision and has not been submitted elsewhere for a degree.



Dr. B.N. Banerjee
Assistant Professor,
Department of Mech. Engg.,
I.I.T., Kanpur.



Dr. A. Ghosh
Professor,
Department of Mech. Engg.,
I.I.T., Kanpur.

ACKNOWLEDGEMENT

It gives me pleasure to express my deep gratitude to Dr. A. Ghosh and Dr. B.N. Banerjee for their constant encouragement and invaluable guidance throughout this work.

I wish to express my thanks to Mr. B.P. Bhartia, Mr. R.M. Jha, Mr. H.P. Sharma and Mr. Pannalal of Manf. Sc. Lab. for their help in fabrication of experimental setup.

I wish to extend my thanks to Mr. Narendra Kumar of TV centre and Mr. S.K. Bhowmick, my friend, for their help in photographic work.

Thanks are also due to a number of friends who have been useful in the course of this work including Mr. Raj Khanna for his neat typing, Mr. B.K. Jain for drawing the figures and Mr. Buddhi Ram for duplicating.

DIPAK B. SHAH

CONTENTS

	Page
CERTIFICATE	... i
ACKNOWLEDGEMENT	... ii
LIST OF FIGURES	... v
ABSTRACT	... vii
CHAPTER-1 INTRODUCTION	
1.1 Impact Phenomenon	... 1
1.1.1 General Characteristics and Types of Impact	... 2
1.1.2 Mechanics of Impact of Rigid Bodies	... 6
1.2 Impact of Rigid Bodies Under No-Slip Condition	... 12
1.2.1 Traditional Procedure for Analysis of Impact	... 13
1.2.2 Recent Proposal for Modification of Procedure	... 18
1.3 Objective and Scope of the Present Work	... 25
CHAPTER-2 EXPERIMENTAL SET-UP AND PROCEDURE	
2.1 Introduction	... 26
2.2 Design and Fabrication of the Test Set-Up	... 26
2.3 Determination of Contact Force Direction During Impact	... 29
2.4 Determination of Velocities before and after Impact	... 33
2.5 Determination of Coefficient of Restitution	... 34
CHAPTER-3 EXPERIMENTAL RESULTS AND DISCUSSIONS	
3.1 C.G. and M.I. of Bodies	... 37
3.2 Contact Force Direction	... 37

	Page
3.3 Velocity Measurement Results	39
3.4 Coefficient of Restitution	52
3.5 Discussion	52
3.5.1 Velocities Obtained Using the Traditional Procedure	52
3.5.2 Velocities Obtained Using the Proposed Procedure	57
CHAPTER-4 CONCLUSIONS	65
REFERENCES	66

LIST OF FIGURES

Figure	Page
1.1 Deformation Vs. Time Diagram	... 4
1.2 Types of Impact	... 5
1.3 Motion of a Particle under the External Force	... 8
1.4 Force Vs. Time Diagram of an Impulse	... 15
1.5 Velocities and Impulses acting during Impact	... 15
1.6 Velocity before and after Impact of a Rough Disc on a Rough Horizontal Surface	... 16
2.1 Schematic Diagram of the Experimental Set-Up	... 27
2.2 Point of Contact of the Bodies during Impact	... 28
2.3 Experimental Set-Up Arrangement for Photographing Fringe Patterns	... 31
2.4 Polarized Light	... 32
2.5 Plane Polariscopic	... 32
2.6 Experimental Set-Up Arrangement for the experiment of Coefficient of Restitution	... 35
3.1 Velocities and Other Dimensions of Impacting Bodies	... 38
3.2 Photography of fringe pattern	... 40
3.3 Illustrations of fringe patterns	... 43
3.4 Photographs of Positions of Body 1 before and after Impact	... 45

Figure		Page
3.5	Schematic Diagram of Positions of Body 1 before and after Impact	... 48
3.6	Schematic Diagram of Heights of Body 1 before and after Impact	... 53
3.7	Determination of Coefficient of Restitution Using Traditional Procedure	... 56
3.8	Determination of Coefficient of Restitution Using Proposed Procedure	... 60

ABSTRACT

Analysis of impact involves detailed study of the complex physical phenomena occurring near the point of contact. The theoretical treatment of the physical processes, local deformation and vibrations of the impacting bodies, produced as a result of the impact requires principles of deformable-body continuum mechanics and mechanical vibrations which renders the mathematical treatment extremely complicated. A classical theory of impact provides a simple procedure to analyse the change in the motion of the impacting bodies considering the bodies as rigid. Recently, a modified procedure has been proposed to analyse the change in motion of the impacting bodies with no-slip condition at the point of contact. In the present work, an experimental analysis of the impact between a moving body and a fixed surface with no-slip condition at the point of contact is carried out. The experimentally obtained results are used to evaluate the results obtained from the existing procedure and the proposed procedure.

CHAPTER-1

INTRODUCTION

1.1. Impact Phenomenon.

The phenomenon of collision of two masses where active and reactive forces of large magnitude are acting on each mass during a relatively very small interval of time is called impact. Such phenomenon is seen taking place in games of billiards, in vehicle accidents, in explosive action of bullet or shell firing from a gun etc. The behaviour of gas can best be described as collisions of gas particles. Other microscopic event which exhibits such behaviour is nuclear reaction in a reactor.

Behaviour of impacting bodies change abruptly after the impact. In addition, the forces produced are of very large magnitude which are usually sufficient to initiate the fracture processes or plastic flow. The impact produces internal stresses, deformation and change of motion in the colliding bodies which may be reversible or irreversible processes. The study of behaviour of materials, macroscopic as well as microscopic to suddenly applied forces helps in understanding the more complex phenomena of fracture initiation and plastic flow at the point of contact.

The study of the physical process involved in an impact is of unsurmountable difficulties. This is so because of the

brevity of the duration and the ignorance of the microscopic aspects involved at the point of contact. The magnitude and the direction of impact change with the shapes of bodies, types of materials and the surface contact characteristics. Models representing the actual physical system must be idealised so as to render them amenable to the theoretical treatment of the problem.

1.1.1. General Characteristics and Types of Impact.

Impacting masses exhibit specific behaviour regarding the physical processes during the impact. These physical processes are concentrated usually at the point of contact and are quite independent from the happenings in the other region of the body. Depending upon the characteristic of the physical behaviour impacts are termed differently. There are three types of impact according to the state of deformation : (i) Perfectly elastic impact, where there is no permanent deformation and energy loss is zero, (ii) Perfectly plastic impact, where the deformation is permanent and energy loss is complete and (iii) Imperfectly elastic impact, where only a part of the maximum deformation is permanent and energy loss is partial. Their characteristics are shown in fig. 1.1. Based on the nature of impacting bodies and their contact position there are four types of impact. They are (i) Direct Impact : If the impact of two nonrotating smooth bodies occurs at a point lying on the line connecting their centres and their initial velocities are in the

same line as that of the common normal, it is called direct impact and the bodies rebound back in the same line after the impact, (ii) Oblique Impact : If the impacting bodies have their initial velocity inclined to the common normal at the point of contact in the above case, it is called oblique impact and the velocity components of bodies perpendicular to the common normal do not change after the impact, (iii) Eccentric Impact : If the impact of two nonrotating bodies occurs at a point not lying on the line connecting their centres, it is called eccentric impact and (iv) Rotational Impact : If the impact causes change only in the angular velocities of the impacting bodies, as in the case of clutch action, it is called rotational impact. The respective examples of above cases are shown in figs. (1.2a), (1.2b), (1.2c) and (1.2d). Again, the impact can be classified according to the contact surface characteristics of impacting bodies. They are (i) Perfectly Smooth Impact : If the surfaces of the impacting bodies are smooth enough so that the coefficient of friction is zero, then the impulse produced acts in a direction normal to the contacting surfaces and (ii) Perfectly rough Impact : If the surfaces of impacting bodies are rough so that the coefficient of friction is infinite, then there is no slip at the contact point. In such cases the resultant impulse is inclined to the common normal.

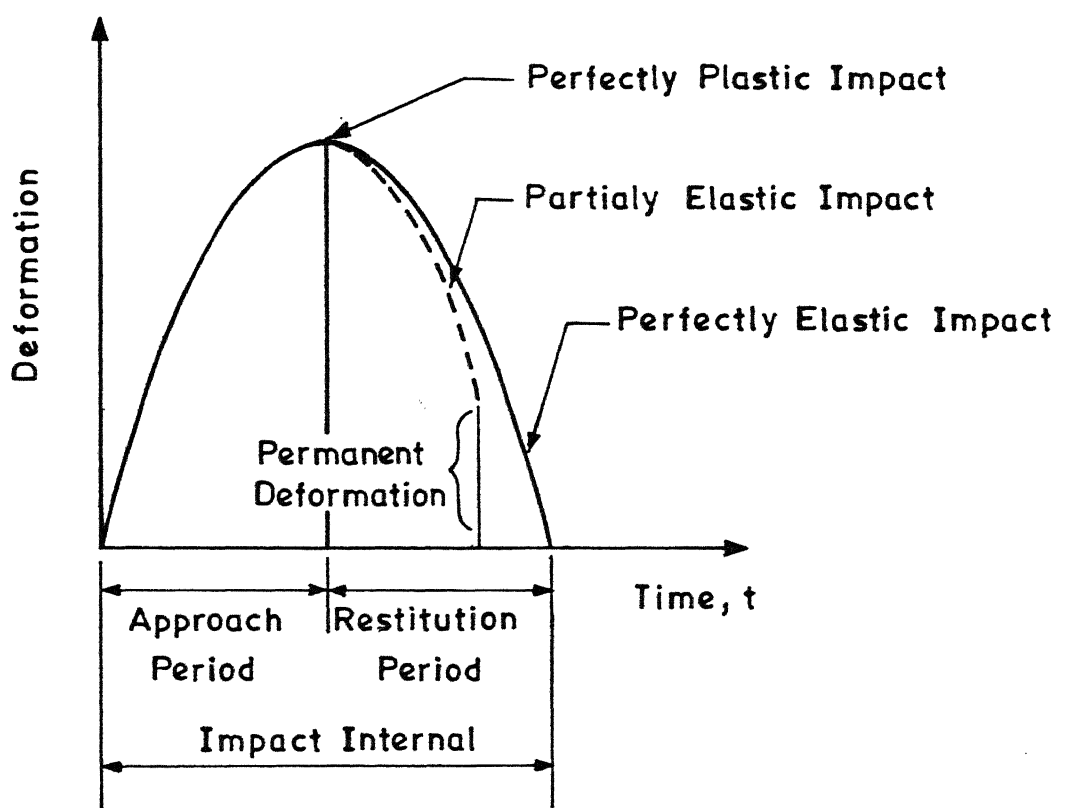
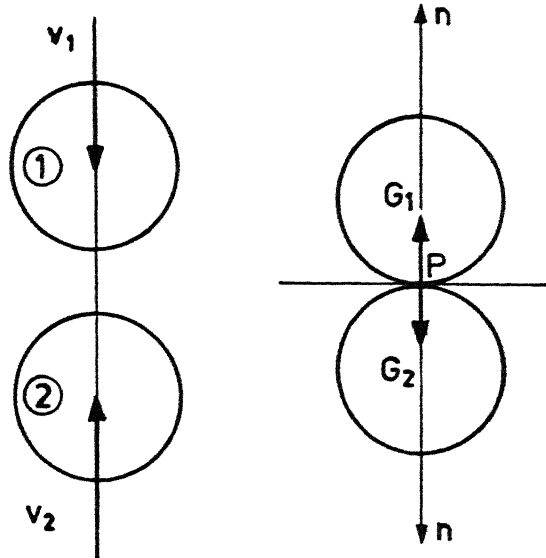
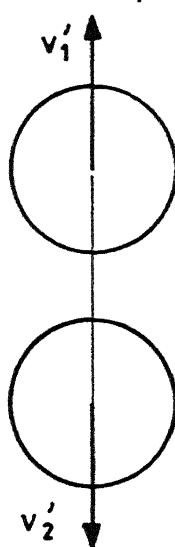


Fig. 1.1 Deformation vs time diagram.

Before Impact

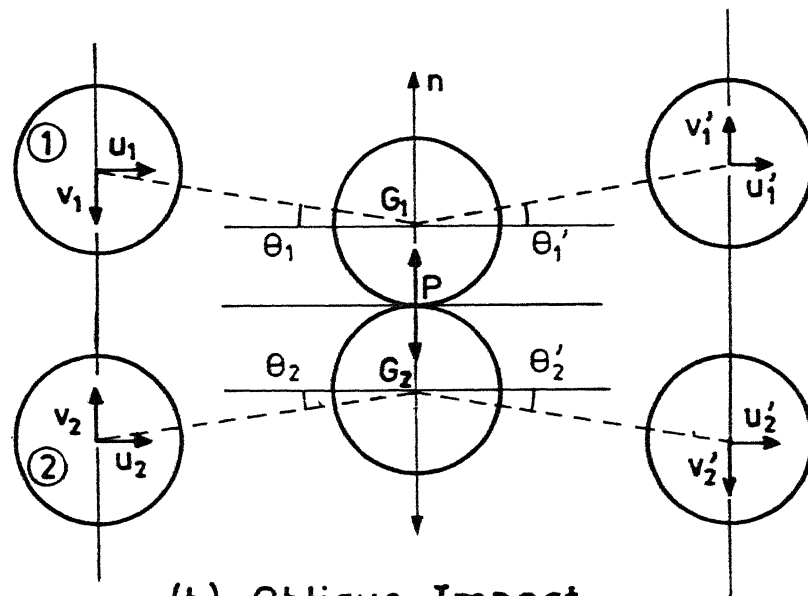


After Impact



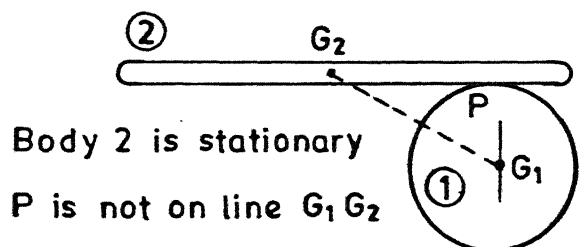
P - Contact point
 n -n-Common norm
 G_1 , G_2 , and P
are on straight
line.

(a) Direct Impact



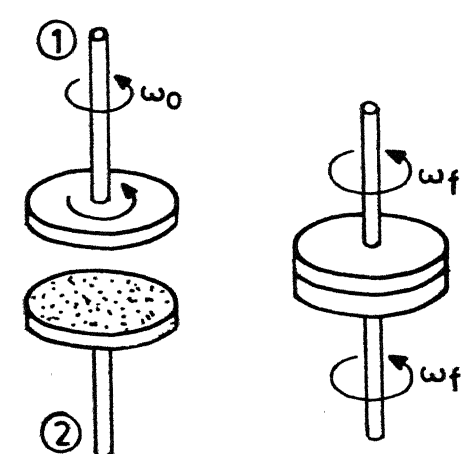
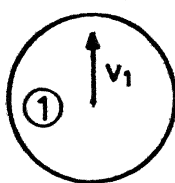
G_1 , G_2 and P
are on straight
line.

(b) Oblique Impact



Body 2 is stationary
P is not on line G_1G_2

(c) Eccentric Impact



Initially Body 2 is stationary
(d) Rotational Impact

Fig. 1.2 Types of impact .

1.1.2. Mechanics of Impact of Rigid Bodies.

The classical theory of impact, called stereomechanics, is based primarily on the laws of impulse-momentum for rigid bodies and is used mainly for finding out the final velocities of the impacting bodies. In the theoretical treatment of the problem of impact of rigid bodies, the impacting bodies are essentially regarded as single mass points having concentrated the mass of the bodies at their centres. Any particle in a rigid body system is assumed to have no displacement with respect to the other particles of the system and all the particles of the system are thus instantaneously subjected to same change of motion as the result of the impact. The laws of linear and angular impulse-momentum for particles can be applied directly to the rigid body system.

The resulting change in motion of the particle due to application of external force over a time interval can be found out from the laws of impulse momentum which are obtained by time integration of the equation of motion of the particle. Consider the curvilinear motion of a particle, P, of mass m in a plane (ref. fig. 1.3) where its position vector r is measured from a fixed point O, its velocity $v = \dot{r}$ is tangent to its path and the resultant ΣF of all forces on mass m is in the direction of acceleration $a = \ddot{v}$. The equation of motion of the particle P can be written as

$$\Sigma F = ma = \frac{d}{dt} (mv) \quad (1.1)$$

The term $\frac{d}{dt} (mv)$ is the time rate of change of linear momentum of the particle. Now if the force is acting on the particle over a small interval of time, as in the case of impact, the linear impulse of the force, \hat{F} , can be obtained by time integration of the equation of motion of the particle as follows (see fig. 1.4) :

$$\int_{t_1}^{t_2} F dt = \int_{t_1}^{t_2} \frac{d}{dt} (mv) dt$$

$$\hat{F} = m (v_2 - v_1) \quad (1.2)$$

where v_1 and v_2 are the velocities of the particles before and after the application of force F . Equation 1.1 signifies that the total linear impulse acting on mass m during the time interval (t_2, t_1) equals the corresponding change in linear momentum of the particle over that time interval.

Similarly, the law of angular impulse-momentum can be obtained. Taking the cross product by multiplying left and right sides of equation 1.1 with the position vector r of the particle P , we have

$$r \times \Sigma F = r \times \frac{d}{dt} (mv)$$

$$= \frac{d}{dt} (r \times mv)$$

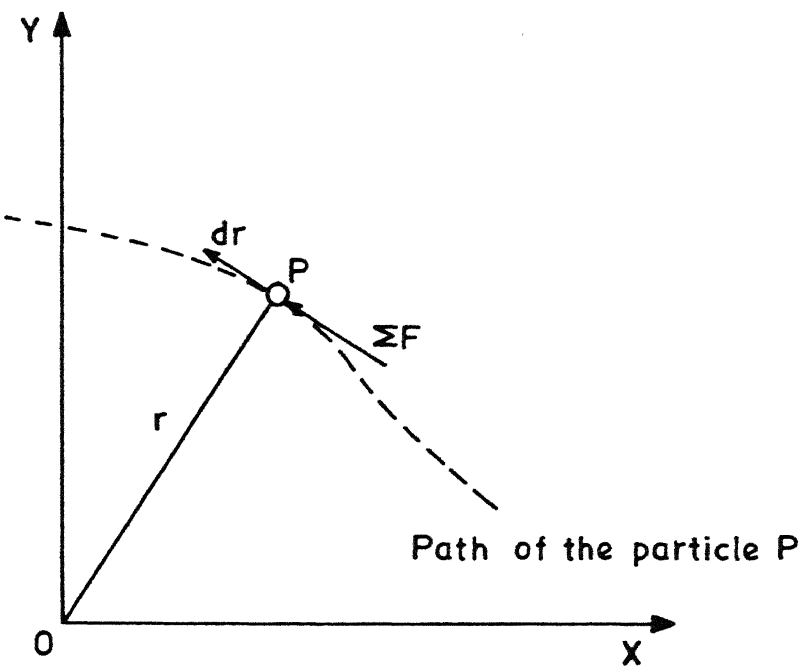


Fig. 1.3 Motion of a particle under the external force.

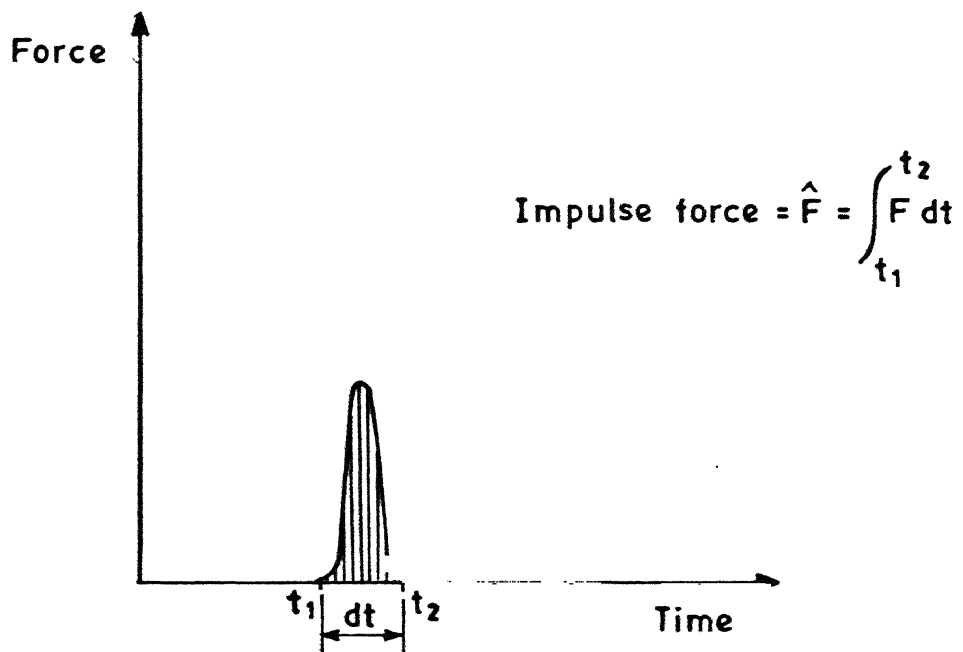


Fig.1.4 Force vs time diagram of an impulse.

If $\mathbf{r} \times \Sigma \mathbf{F}$ and $\mathbf{r} \times \mathbf{mv}$ are denoted by M and H respectively, we have

$$M = \dot{H}$$

where M is the moment of the resultant forces about the fixed point O and H is the moment of momentum, or angular momentum, of particle P about the fixed point O.

Now the time integration of the resultant moment about the fixed point O of the forces acting on the particle during the time interval (t_2, t_1) gives the angular impulse M .

$$\hat{M} = \int_{t_1}^{t_2} M dt = \int_{t_1}^{t_2} \dot{H} dt = H_2 - H_1 \quad (1.3)$$

Equation 1.3 signifies that the total angular impulse of the resultant forces acting on mass m about the fixed point O during the time interval (t_2, t_1) equals the change in angular momentum of the particle about the same point over that time interval. The above obtained laws of impulse-momentum for the particles can be used to write similar laws for the rigid bodies in plane motion.

Suppose the external force acting on a rigid body is a function of time, and suppose we know the initial configuration of the rigid body i.e. the position and velocity of the rigid body at some instant of time, then subsequent motion of the mass centre of rigid body can be described by time integration of linear and angular impulse-momentum laws.

$$\begin{aligned}
 \text{Linear impulse } \hat{F} &= \int_{t_1}^{t_2} F \, dt \\
 &= m (v_2 - v_1) \\
 &= \Delta (mv)
 \end{aligned}$$

$\Delta (mv)$ is the change in linear momentum of the rigid body as the result of the linear impulse \hat{F} .

Similarly,

$$\begin{aligned}
 \text{Angular impulse } \hat{M} &= \int_{t_1}^{t_2} M \, dt \\
 &= \Delta H \\
 &= \Delta (I\omega)
 \end{aligned}$$

$\Delta (I\omega)$ is the change in angular momentum of the rigid body as the result of the angular impulse \hat{M} .

The application of the impulse-momentum relationships to the problem of impacting of rigid bodies is suitable because of the relatively large forces produced during the relatively small impact interval. Forces produced as the result of the impact are called impulsive forces and are responsible for the subsequent change in the motion of the impacting rigid bodies.

The impact of two rigid bodies can be considered as an isolated system, and so the impulsive forces produced as the result of the impact are internal to the system. In absence of any external force on the system, the total linear momentum of the system of two rigid bodies remains constant and only the

linear momentum transfer of a rigid body occurs. Similarly, the total angular momentum of the system of two impacting rigid bodies remains constant, and so any couples applied to the rigid body as the result of the impact contribute to the angular impulse only but not to the linear impulse.

The perfectly elastic impact of two bodies i.e. the mechanical energy of the system of two impacting bodies is conserved, provides required additional relation together with principles of conservation of linear and angular momentum to find out the final velocities of the bodies after the impact.

Above formulations are the most idealised concepts of the physical phenomenon of the impact because in reality when two bodies collide, some local deformation, which may be permanent, occurs at the point of contact. In actual physical phenomenon of impact, some portion of the initial kinetic energy of the bodies is always lost in the form of heat dissipation, sound, and some portion is transferred into the vibrations of the impacting bodies. The detailed description and analysis of the physical processes involved at the point of contact would call for the principles of deformable-body continuum mechanics and mechanical vibrations. In classical theory of impact, a coefficient of restitution is incorporated to approximate the complex processes involved at the point of contact. Coefficient of restitution is defined as the ratio of the relative velocity of

departure to the relative velocity of approach of the impacting bodies at the contact point along the common normal. The local deformation at the point of contact is envisaged as consisting of two subintervals as shown in fig. 1.1. The approach period extends from the instant of physical contact of two bodies to the point of maximum compression, followed by a restitution period lasting to the instant of separation of two bodies. The value of $e = 1$ and $e = 0$ correspond to the respective idealised concepts of perfectly elastic impact when the over all change in the mechanical energy of the system is zero and perfectly plastic impact when the loss of mechanical energy of the system is complete and the bodies do not separate after the impact. In practice, the value of e generally lies inbetween these two extreme situations and its appropriate value for any specific case depends upon the materials, initial velocities, and shapes of contacting surfaces and is determined by experiments.

1.2. Impact of Rigid Bodies under No Slip Condition .

Impact of rigid bodies under no slip condition at their point of contact has been discussed in many standard books on dynamics. The resultant impact produced during impact should not necessarily act along the normal to the contact surfaces. Unlike the impact of smooth bodies, an impulse tangential to the surfaces is contact is produced.

1.2.1. Traditional Procedure for Analysis of Impact .

In the traditional procedure, the impact phenomenon is considered to be instantaneous at the point of contact and the local deformation produced at the contact point is approximated by using the concept of coefficient of restitution. The magnitude of impact is found out from the initial and final states of velocities of the impacting bodies. The procedure available in the books [1-5], to determine the velocities of two rigid bodies after the impact, is as follows.

Fig. 1.5a shows two impacting bodies (with G_1 and G_2 as their mass centres) just before the impact. The body 1 has u_1 , and v_1 linear velocity components and ω_1 angular velocity about its C.G. G_1 . Similarly, body 2 has u_2 , and v_2 linear velocity components and ω_2 angular velocity about its C.G. G_2 . Generally, the coefficient of restituion (e) is prescribed for the material, or alternatively determined by the experiments.

To find out the six unknown velocity components (u_1' , v_1' , ω_1' of body 1 and u_2' , v_2' , ω_2' of body 2) just after the impact, six equations are obtained as follows :

- (i) Two equations are obtained by conserving the total momentum of the two bodies in the u and v directions.
- (ii) One equation is obtained by expressing the relative departure velocity components of the contact point along the common normal as a product of the coefficient of resti-

tution and relative approach velocity component of contacting point along the common normal.

- (iii) One equation is obtained by conserving the total angular momentum of the system.
- (iv) Two equations are obtained by relating u_1' , v_1' , ω_1' of body 1 and u_2' , v_2' , ω_2' of body 2 considering the two bodies instantaneously hinged at the contacting point A as there is no slip.

Above mentioned procedure can be demonstrated by considering a simple example. As shown in fig. 1.6a, a rigid body of mass m , diametral moment of inertia I and radius r drops on a perfectly rough horizontal surface with a linear velocity v and angular velocity ω about its C.G. G. The body has u' and v' linear velocity components and w' angular velocity just after the impact as shown in the fig. 1.6b. Three equations required to find out three unknown velocities (u' , v' and ω') just after the impact can be written as follows.

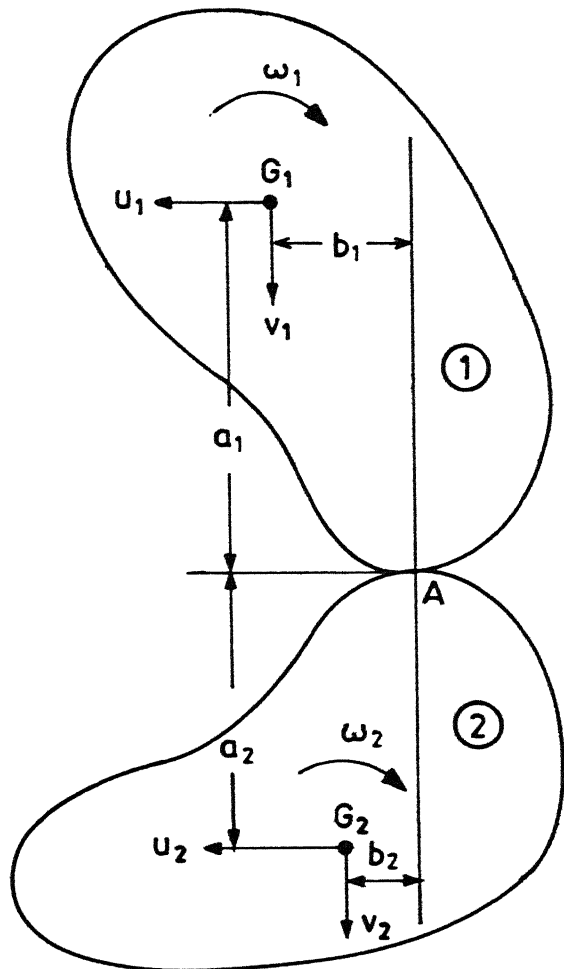
- (i) Impact is considered to have no slip condition at the point of contact. This gives,

$$u' = \omega' r$$

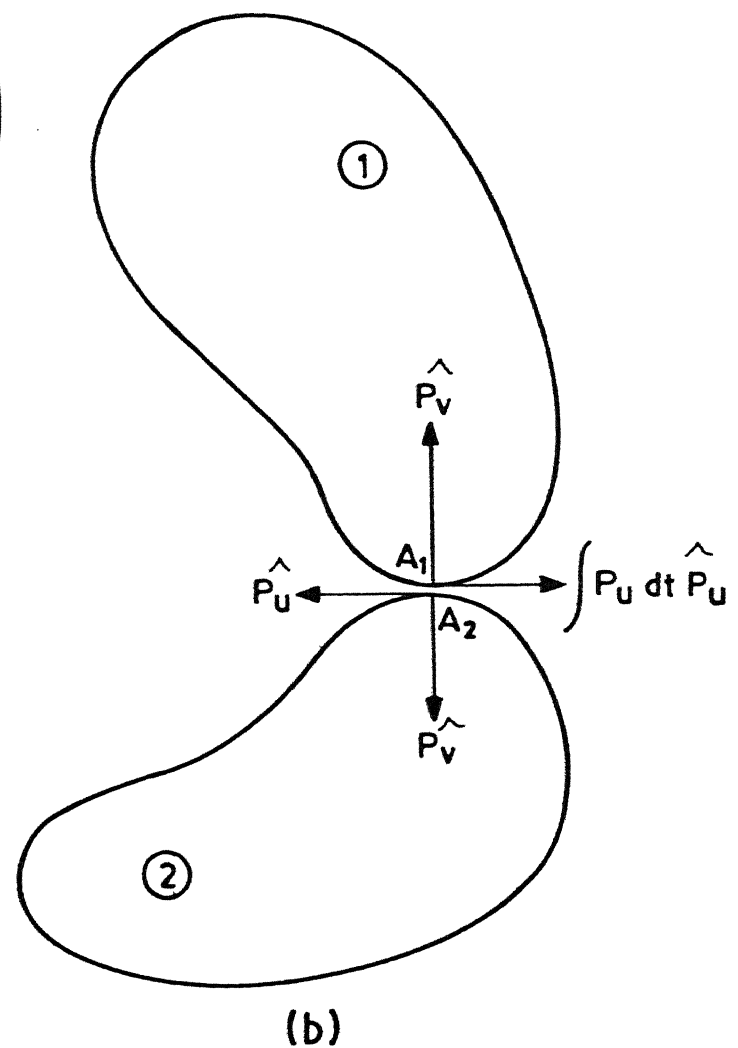
- (ii) Considering the impact to be imperfectly elastic, we have,

$$v' = ev \quad \text{where } e \text{ is the coefficient of restitution.}$$

- (iii) Conserving the total angular momentum of the system about



(a)



(b)

Fig. 1.5 Velocities and impulses acting during impact.

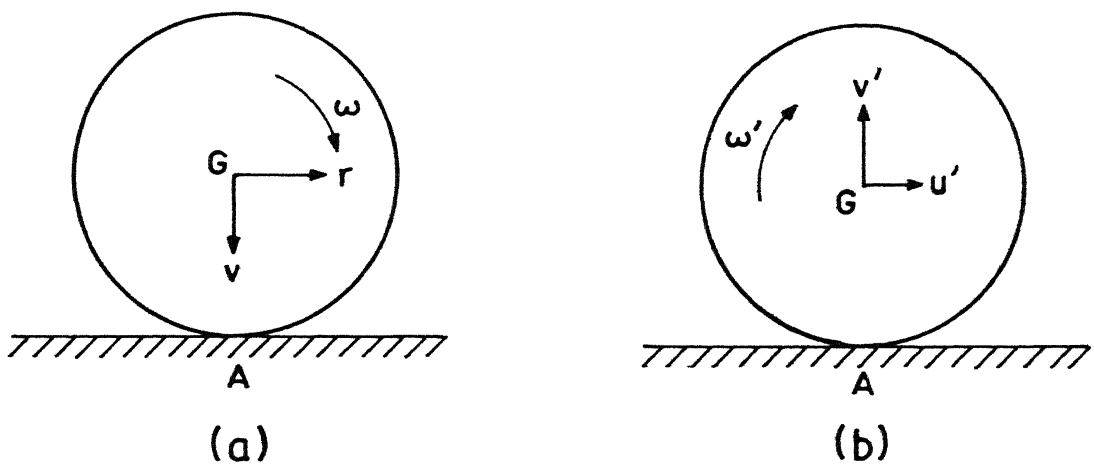


Fig. 1.6 Velocity before and after impact of a rough sphere on a rough horizontal surface.

the contact point A, we have

$$I\omega = I\omega' + mr^2\omega'$$

Solving above three equations, we get the final velocities of mass m just after the impact. They are

$$u' = \frac{I\omega r}{I + mr^2} \quad (1.4a)$$

$$v' = ev \quad (1.4b)$$

$$\text{and } \omega' = \frac{I\omega}{I + mr^2} \quad (1.4c)$$

If the impact has to be perfectly elastic i.e. the mechanical energy loss of the system is zero during the impact, the final velocities of the body after the impact can be obtained by putting $e = 1$ in above equations. The overall mechanical energy of the system should be conserved for the perfectly elastic impact and this can be checked by equating the initial and final kinetic energy of the system.

The initial K.E. of the system before the impact is

$$T_i = \frac{1}{2} mv^2 + \frac{1}{2} I\omega^2 \quad (1.5a)$$

and the final K.E. of the system after the impact is

$$T_f = \frac{1}{2} mv'^2 + \frac{1}{2} \frac{I^2}{(I + mr^2)^2} \omega'^2 \quad (1.5b)$$

The examination of eq. 1.5a and eq. 1.5b indicates that the

energy of the system is less after the impact i.e. some energy is lost during the impact. This is contradicting the principle of conservation of mechanical energy of the system for perfectly elastic impact. The fallacy in the analysis is explained in the section 1.2.2.

1.2.2. Recent Proposal For Modification of the Procedure.

Ghosh¹ has given an improved procedure for dynamical analysis of the impact phenomenon considering the fact that the contacting particles have finite deformation velocities with respect to the rest of the otherwise rigid bodies. In the traditional procedure, the impact is considered to be instantaneous, and so the mass centres of impacting bodies and the respective contacting particles are assumed to have no relative displacement during the impact. The macroscopic examination near the contact point reveals that there is always some local deformation at the contact point. After the initial contact of two bodies, the mass centres of two bodies still continue to approach each other till they reach maximum deformation, and so even before the physical contact between two contacting particles breaks, the mass centres of the bodies would have acquired velocities. This shows that the contacting particle and the respective mass centre can not be treated as two particles on the rigid body during the impact interval except at the instant

¹ Since the work is not published, the procedure proposed by him is presented here in detail.

of maximum local deformation. At the threshold of the periods of approach and restitution when the local deformation is maximum, the rate of deformation is zero and so the impacting bodies including the contacting particles can be considered as perfectly rigid. The analysis, given by Ghosh, is based on this instant to derive equations relating the initial and final velocities of impacting bodies rather than the instant corresponding to the end of the impact.

Fig. 1.5a shows two bodies 1 and 2 at the instant when impact starts. The masses and the moment of inertia about the axes passing through the mass centres G_1 and G_2 are m_1 , m_2 , I_1 , and I_2 respectively. Linear velocity components, angular velocities and other dimensions are shown in the figure.

As the impact is considered to have no slip condition at the contact point A, contacting particles must have zero relative velocity. The resultant impulse acting on the bodies 1 and 2 during the period of approach is resolved into components as shown in fig. 1.5b. Again as the resultant deformation is resolved into normal and shear components, the periods of deformation and restitution for both the normal and shear directions are same. The components of mass centre velocities and the angular velocities at the threshold of the periods of deformation and restitution can be written as follows :

$$\bar{u}_1 = u_1 - \frac{\Delta P_u}{m_1} \quad (1.6a)$$

$$\bar{v}_1 = v_1 - \frac{\Delta P_v}{m_1} \quad (1.6b)$$

$$\bar{\omega}_1 = \omega_1 - \frac{1}{I_1} (a_1 \frac{\Delta P_u}{m_1} + b_1 \frac{\Delta P_v}{m_1}) \quad (1.6c)$$

$$\bar{u}_2 = u_2 + \frac{\Delta P_u}{m_2} \quad (1.6d)$$

$$\bar{v}_2 = v_2 + \frac{\Delta P_v}{m_2} \quad (1.6e)$$

$$\bar{\omega}_2 = \omega_2 - \frac{1}{I_2} (a_2 \frac{\Delta P_u}{m_2} - b_2 \frac{\Delta P_v}{m_2}) \quad (1.6f)$$

where \bar{u}_1 , \bar{v}_1 , \bar{u}_2 , \bar{v}_2 , $\bar{\omega}_1$ and $\bar{\omega}_2$ are velocities at the end of deformation, P_u and P_v are the impulse in the normal and shear directions during the period of deformation.

Since the two bodies can be considered to be perfectly rigid at the threshold of the periods of deformation and restitution the velocity components of the contacting particles on two bodies at A can be written as

$$\bar{u}_{A1} = \bar{u}_1 + \bar{\omega}_1 a_1 \quad (1.7a)$$

$$\bar{v}_{A1} = \bar{v}_1 + \bar{\omega}_1 b_1 \quad (1.7b)$$

$$\bar{u}_{A2} = \bar{u}_2 - \bar{\omega}_2 a_2 \quad (1.7c)$$

$$\bar{v}_{A2} = \bar{v}_2 + \bar{\omega}_2 b_2 \quad (1.7d)$$

If $\overset{\Delta}{R}_u$ and $\overset{\Delta}{R}_v$ are the components of the resultant impulse during the period of restitution, the components of velocities of mass centres G_1 and G_2 and angular velocities at the end of impact can be written as follows :

$$u'_1 = \bar{u}_1 - \frac{\overset{\Delta}{R}_u}{m_1} \quad (1.8a)$$

$$v'_1 = \bar{v}_1 - \frac{\overset{\Delta}{R}_v}{m_1} \quad (1.8b)$$

$$\omega'_1 = \bar{\omega}_1 - \frac{1}{I_1} (a_1 \overset{\Delta}{R}_u + b_1 \overset{\Delta}{R}_v) \quad (1.8c)$$

$$u'_2 = \bar{u}_2 - \frac{\overset{\Delta}{R}_u}{m_2} \quad (1.8d)$$

$$v'_2 = \bar{v}_2 - \frac{\overset{\Delta}{R}_v}{m_2} \quad (1.8e)$$

$$\omega'_2 = \bar{\omega}_2 - \frac{1}{I_2} (a_2 \overset{\Delta}{R}_u - b_2 \overset{\Delta}{R}_v) \quad (1.8f)$$

The primed quantities in the above equations represent the velocities at the end of impact.

Since there is no-slip condition at the point of contact, the contacting particles A_1 and A_2 must have zero relative velocity i.e. $\bar{u}_{A1} = \bar{u}_{A2}$ and $\bar{v}_{A1} = \bar{v}_{A2}$. From equations (1.6) and (1.7), we get the following relations using above conditions.

$$(u_1 + \omega_1 a_1) - (u_2 - \omega_2 a_2) = \left(\frac{1}{m_1} + \frac{1}{m_2} + \frac{a_1^2}{I_1} + \frac{a_2^2}{I_2} \right) \overset{\Delta}{P}_u$$

$$+ \left(\frac{a_1 b_1}{I_1} - \frac{a_2 b_2}{I_2} \right) \overset{\Delta}{P}_v ; \quad (1.9a)$$

$$(v_1 + \omega_1 b_1) - (v_2 + \omega_2 b_2) = \left(\frac{a_1 b_1}{I_1} - \frac{a_2 b_2}{I_2} \right) \dot{P}_u^A + \left(\frac{1}{m_1} + \frac{1}{m_2} + \frac{b_1^2}{I_1} + \frac{b_2^2}{I_2} \right) \dot{P}_v^A \quad (1.9b)$$

The velocities at the end of impact can be expressed in terms of the velocities at beginning of the impact by using eq. 1.6 in eq. 1.8 .

$$u_1' = u_1 - \frac{1}{m_1} (\dot{P}_u^A + \dot{R}_u^A) \quad (1.9a)$$

$$v_1' = v_1 - \frac{1}{m_1} (\dot{P}_v^A + \dot{R}_v^A) \quad (1.9b)$$

$$\omega_1' = \omega_1 - \frac{1}{I_1} [a_1 (\dot{P}_u^A + \dot{R}_u^A) + b_1 (\dot{P}_v^A + \dot{R}_v^A)] \quad (1.9c)$$

$$u_2' = u_2 + \frac{1}{m_2} (\dot{P}_u^A + \dot{R}_u^A) \quad (1.9d)$$

$$v_2' = v_2 + \frac{1}{m_2} (\dot{P}_v^A + \dot{R}_v^A) \quad (1.9e)$$

$$\omega_2' = \omega_2 - \frac{1}{I_2} [a_2 (\dot{P}_u^A + \dot{R}_u^A) - b_2 (\dot{P}_v^A + \dot{R}_v^A)] \quad (1.9f)$$

If the components of the velocity of approach of body 1 with respect to body 2 at A are given by u_A^a and v_A^a , then from eqs. 1.7 and 1.9 , the following equations can be written.

$$\lambda_1 \dot{P}_u^A + \lambda_0 \dot{P}_v^A = u_A^a \quad (1.10a)$$

$$\lambda_0 \dot{P}_u^A + \lambda_2 \dot{P}_v^A = v_A^a \quad (1.10b)$$

$$\text{where } u_A^a = (u_1 + \omega_1 a_1) - (u_2 - \omega_2 a_2),$$

$$v_A^a = (v_1 + \omega_1 b_1) - (v_2 + \omega_2 b_2),$$

$$\lambda_o = \frac{a_1 b_1}{I_1} - \frac{a_2 b_2}{I_2},$$

$$\lambda_1 = \frac{1}{m_1} + \frac{1}{m_2} + \frac{a_1^2}{I_1} + \frac{a_2^2}{I_2}$$

$$\text{and } \lambda_2 = \frac{1}{m_1} + \frac{1}{m_2} + \frac{b_1^2}{I_1} + \frac{b_2^2}{I_2}$$

Now by solving eq. 1.10a and 1.10b, the expressions for the components of impulse in normal and shear directions during the period of deformation can be obtained. They are

$$\hat{P}_u = \frac{\lambda_2 u_A^a - \lambda_o v_A^a}{\lambda_1 \lambda_2 - \lambda_o^2} \quad (1.11a)$$

$$\text{and } \hat{P}_v = \frac{\lambda_1 v_A^a - \lambda_o u_A^a}{\lambda_1 \lambda_2 - \lambda_o^2} \quad (1.11b)$$

If the resultant impact direction during the periods of deformation and restitution is assumed to remain same, which signifies that the energy loss factors both in the normal and shear directions are same, then

$$\frac{\hat{R}_u}{\hat{P}_u} = \frac{\hat{R}_v}{\hat{P}_v} = e \quad (1.12)$$

where e is defined as the coefficient of restitution.

Now from eqs. 1.9 and 1.12, the final velocities of the mass centres in the terms of their initial velocities can be expressed as follows :

$$u_1' = u_1 - \frac{1+e}{m_1} \cdot \frac{\Delta p}{\rho_u} \quad (1.13a)$$

$$v_1' = v_1 - \frac{1+e}{m_1} \cdot \frac{\Delta p}{\rho_v} \quad (1.13b)$$

$$\omega_1' = \omega_1 - \frac{1+e}{I_1} (a_1 \frac{\Delta p}{\rho_u} + b_1 \frac{\Delta p}{\rho_v}) \quad (1.13c)$$

$$u_2' = u_2 + \frac{1+e}{m_2} \frac{\Delta p}{\rho_u} \quad (1.13d)$$

$$v_2' = v_2 + \frac{1+e}{m_2} \frac{\Delta p}{\rho_v} \quad (1.13e)$$

$$\omega_2' = \omega_2 - \frac{1+e}{I_2} (a_2 \frac{\Delta p}{\rho_u} - b_2 \frac{\Delta p}{\rho_v}) \quad (1.13f)$$

If u_A^r and v_A^r be the components of the velocity of recession of body 1 with respect to body 2 at A (after the impact is just over and the whole body including the contacting particle can be again considered to be a rigid body), then eqs. 1.11 and 1.13 yield the following relations :

$$u_A^r = e u_A^a \quad (1.14a)$$

$$v_A^r = e v_A^a \quad (1.14b)$$

The eqs. 1.14a and 1.14b imply that e is also equal to the ratio of the receding and the approaching velocities at the

contact point.

1.3. Objective and Scope of the Present Work .

The primary objective of this work is to fabricate an experimental set up and study the impact phenomenon between a fixed surface and a disc administering no slip condition at their contact point. Using the traditional procedure the theoretical analysis, regarding the bodies as rigid, is done by approximating the local deformation process with the concepts of the coefficient of restitution. The theoretical analysis is also done by considering the bodies as rigid at the threshold of the periods of approach and restitution as mentioned in sec. 1.2.2. A comparative study of analysis of experimental and theoretical results is to be obtained. Other objective was to find out the contact force direction during the period of impact using photoelasticity and high speed movie photography technique.

CHAPTER-2

EXPERIMENTAL SET-UP AND PROCEDURE

2.1. Introduction :

In view of the discussion in the previous chapter, different experiments were carried out. Two types of experiments were conducted : (i) to measure the velocity components and angular velocity of the moving body before and after the impact and (ii) to determine the direction of contact force during the whole action of the impact.

The experiment required the no-slip condition at the point of contact between the two impacting bodies. The choice of material of the bodies was limited by the availability and requirement of a material which should possess photoelastic properties in addition to exhibition of good elastic behaviour on the application of the impact. The material of the bodies was chosen to be U-32 rubber.

2.2. Design and Fabrication of the Test Set-up :

The schematic diagram of the experimental setup is shown in fig. 2.1. One body (body 2) is kept stationary, while the other body (body 1) falls freely on the stationary body from above. The test setup consists of the following parts :

- (i) Base
- (ii) Glass panels

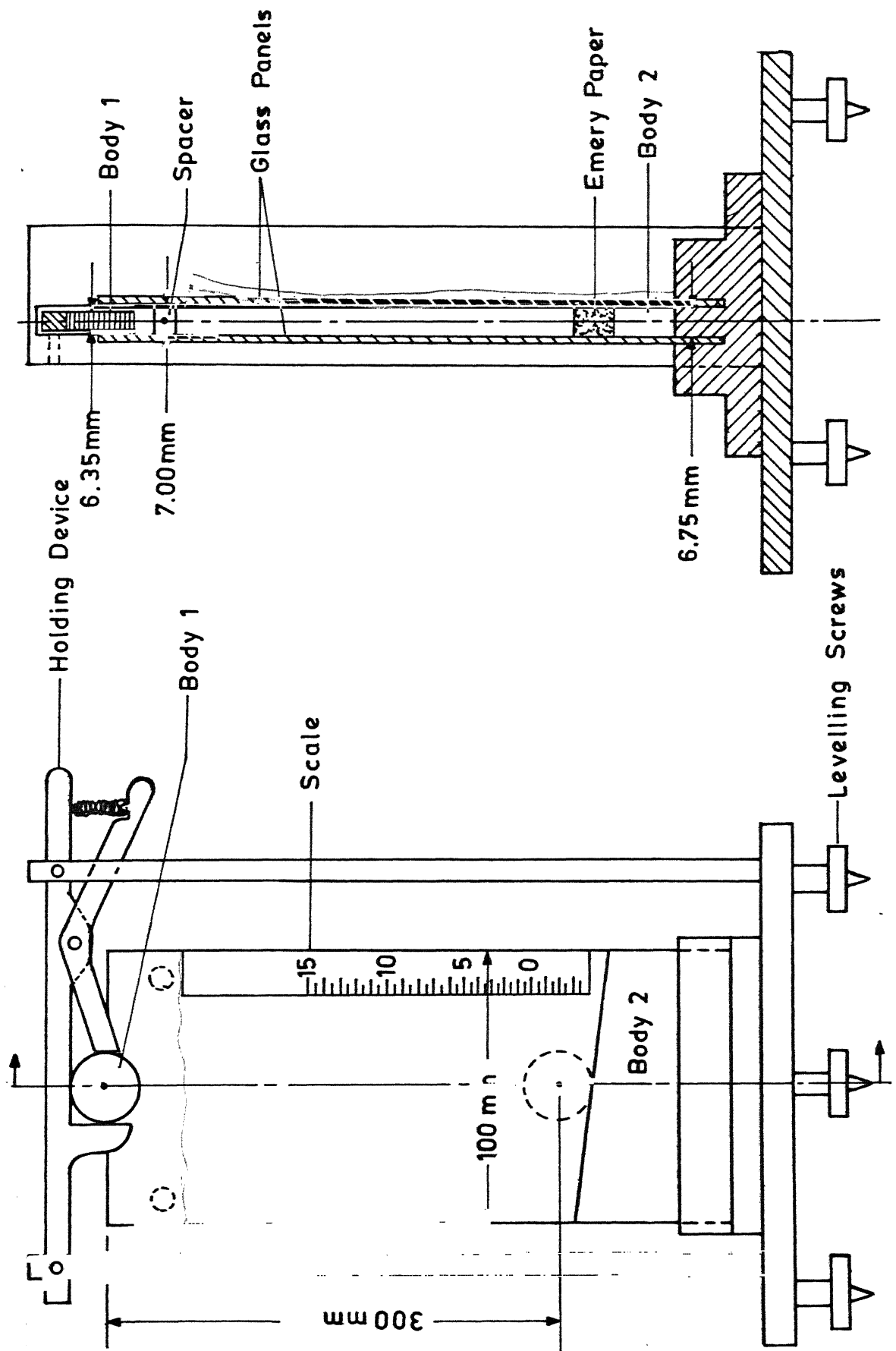


Fig. 2.1 Schematic diagram of the experimental set-up.

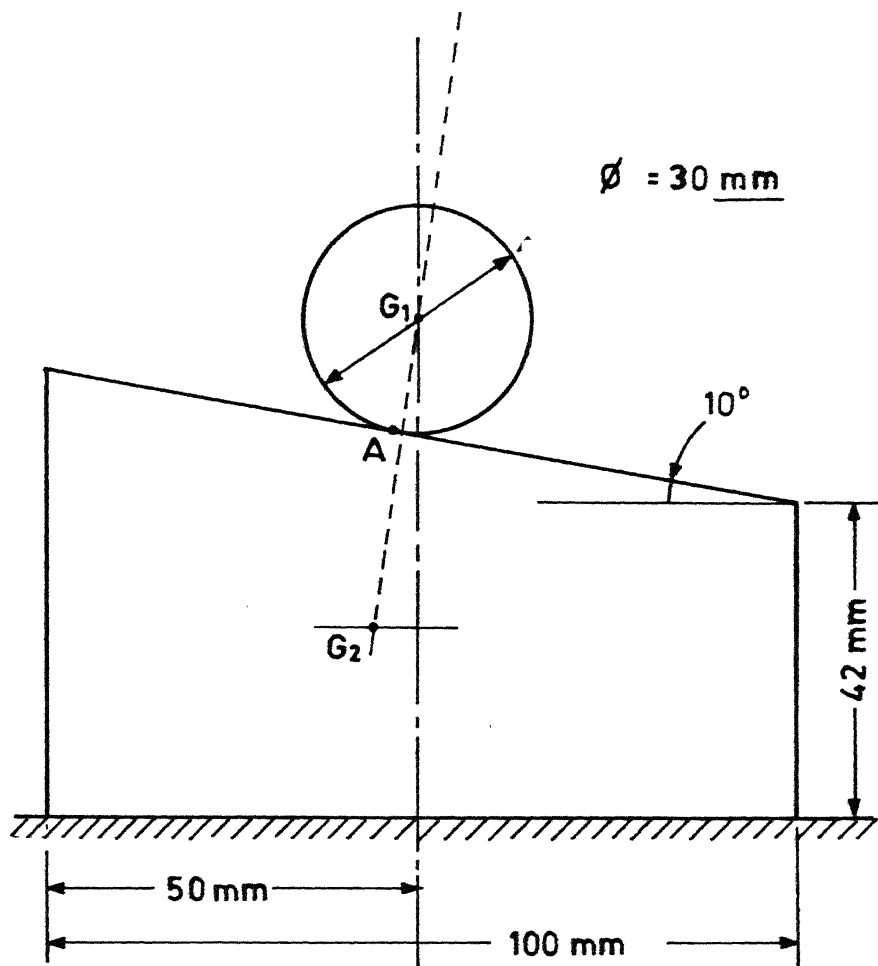


Fig. 2.2 Point of contact of the bodies during impact.

- (iii) Body 1 and Body 2
- (iv) Holding device for releasing body 1
- (v) High speed camera

The body 1 is a disc cut from a 1/4 inch thick sheet of U-32 rubber. While the body 2 is of the same thickness, it is cut to make an angle of 10° with the horizontal plane of the base. Because of the inclined surface of body 2, the point of contact between the two bodies, A, does not lie on the line connecting their respective mass centres G_1 and G_2 (ref. fig. 2.2), and so angular momentum is imparted to the body 1 as a result of the impact action.

The base of the setup is fabricated from perspex. The fabrication of the test setup required a high degree of precision to restrict the lateral displacement of body 2 though allowing body 1 to drop freely without touching the sides of glass panels. The base is provided with levelling screws to make it absolutely horizontal and hence the body 1 falls in the plane of body 2. The inclined surface of the body 2 on which body 1 drops is lined with emery paper to restrict any slip at the point of contact.

2.3 Determination of Contact Force Direction during Impact :

The experiment is carried out to check the direction of impulse of forces produced at the point of contact during the intervals of approach and restitution. The layout for the

experiment is shown in fig. 2.3. The experiment is based on the principles of photoelasticity.

The actual working of the principles of photoelasticity requires a polariscope which consists of two polarizing filters, photoelastic medium and a light source. The polarizing filters have the property to transmit the ordinary light waves, which generally propagate in random directions, only parallel to their axis of polarization and thus two polarizing filters kept in series with their axis of polarization perpendicular to each other produce dark field (see fig. 2.4). When a photoelastic medium put inbetween two polarizing filters is stressed, and the emerging plane polarized light from the polarizer falls on some point in the medium, the incident light is split into two polarised components in the directions of the axis of principal stresses (σ_1, σ_2) at that point [6]. These two waves of light travel at different speed in the photoealstic medium and suffer a relative retardation on emerging from the medium. When these two waves of light pass through the second polarizing filter, called analyzer, only those components of two waves are transmitted through the analyzer which are parallel to its axis of polarization and the transmitted components combine to give a resultant light wave. (see fig. 2.5). Thus every point on the photoelastic medium, where either axis of principal stresses is aligned with the axis of polarization of polarizer, looks dark

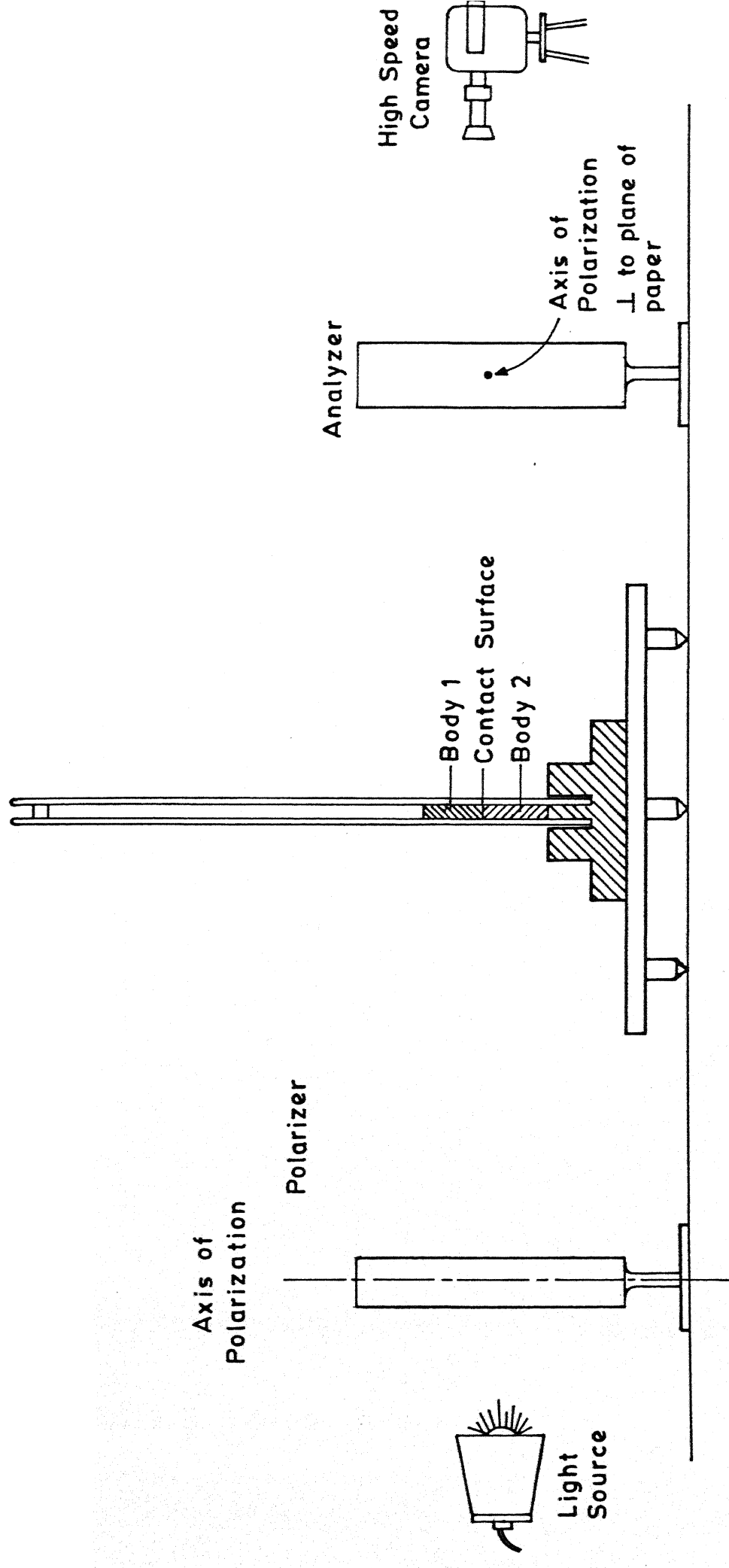
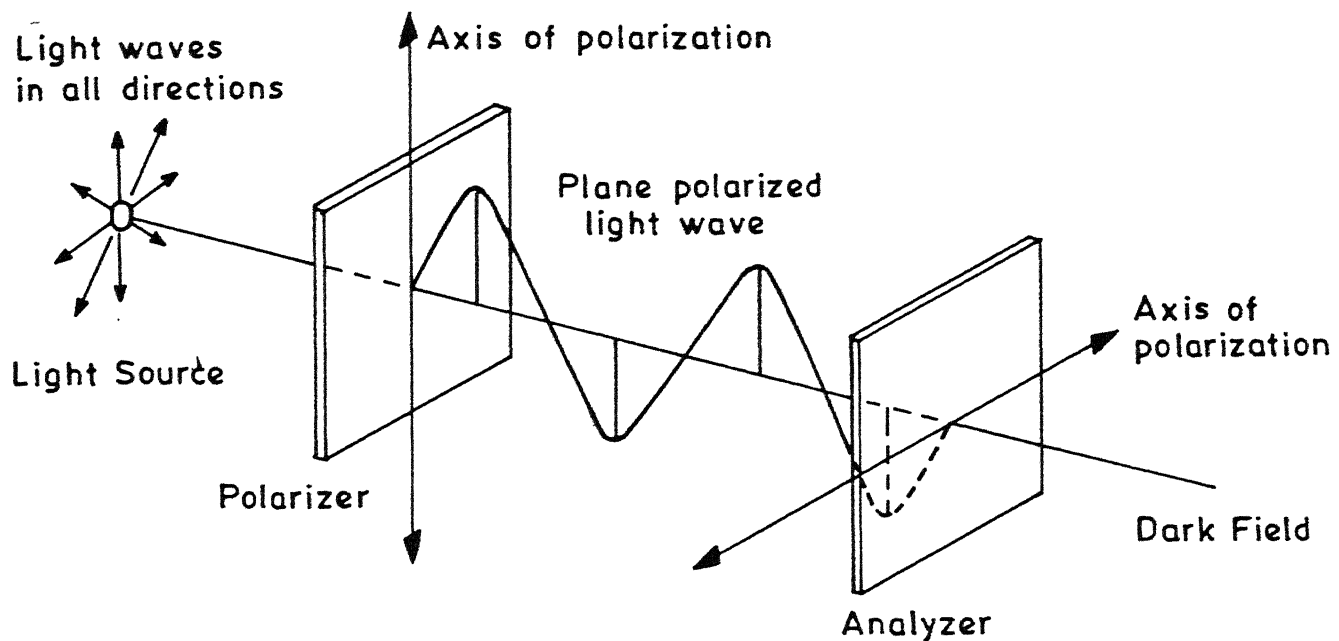


Fig. 2.3 Experimental set up arrangement for photographing fringe patterns.



Axis of Polarizer and Analyzer crossed at 90°

Fig. 2.4 Polarized light

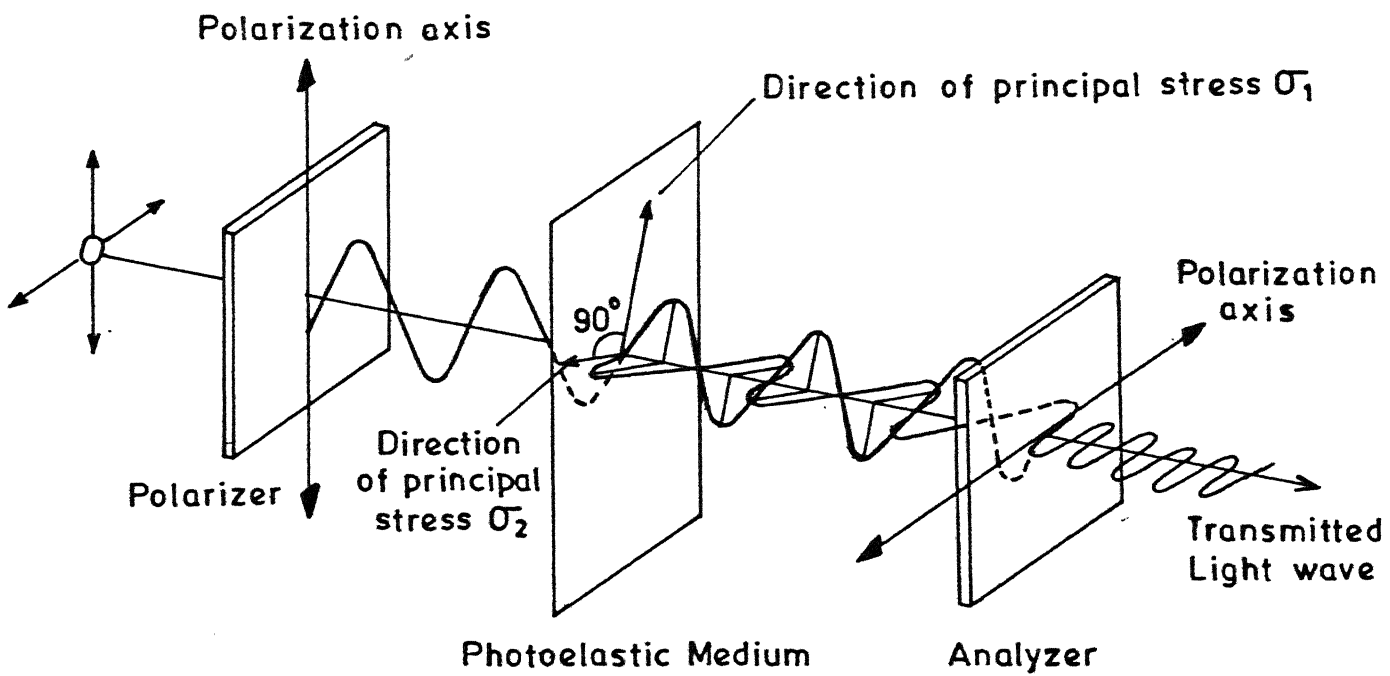


Fig. 2.5 Plane Polariscopic.

on looking into the analyzer. The lines joining all such points are called isoclinics and irrespective of the light source used, they are seen as black fringes on the analyzer.

The impulsive forces produced during the impact interval setup a dynamic stress field in the bodies near the contact point. The photographs of the fringe pattern corresponding to the stress field produced in body 2 near the contact point A are captured by a high speed movie camera. As the contact of two bodies lasts for a very short period of time, the camera is switched on slightly in advance to acquire the desired high film speed, and so take a sufficient number of photographs of the fringe pattern. The film speed at the time of impact is 1400 frames per second and six photographs of the fringe pattern occurring in the course of the impact could be captured.

2.4 Determination of Velocity before and after the Impact :

Impact causes a sudden change in the motion of the impacting bodies. The experiment is carried out to find out the velocities of body 1 before and after the impact. Body 2 is rested on the base and is tightly held inbetween two glass panels to restrict its lateral motion during the impact. Care is taken to keep the point of contact of the two bodies the same each time the body 1 is dropped on body 2 and this is achieved by dropping the body 1 from a holding device.

The photographs of positions of body 1 before and after

the impact are captured by a high speed movie camera. The camera facing side of body 1 is painted black, and a white radial line is painted over, to measure the angular rotation of body 1 about its mass centre in each photograph and a linear scale is mounted on the glass panel to read the linear displacement of body 1 in each photograph. The viewfinder of the camera is adjusted at the point of contact of the two bodies and without shifting the viewfinder the photographs of body 1 before and after the impact are taken. The camera is operated at 64 frames per second and so the linear displacement of body 1 and its angular rotation about the mass centre during each time interval of $1/64$ sec. is recorded. The experiment is repeated several times to check the repeatability of the results.

2.5 Determination of Coefficient of Restitution(e) :

The experiment is carried out to determine the coefficient of restitution for the material of impacting bodies. Fig. 2.6 shows the schematic diagram of the arrangement of the experimental set-up. As shown in the figure, body 1 is dropped freely on to body 2 which is tightly held between two glass panels. The contacting surface of the body 2 is lined with a thin emery paper to keep the surface characteristic the same.

The body 1 which is a disc is dropped from a fixed height (H). Since the contacting surface of body 2 is horizontal, body 1 bounces off vertically upward to some height (h) after

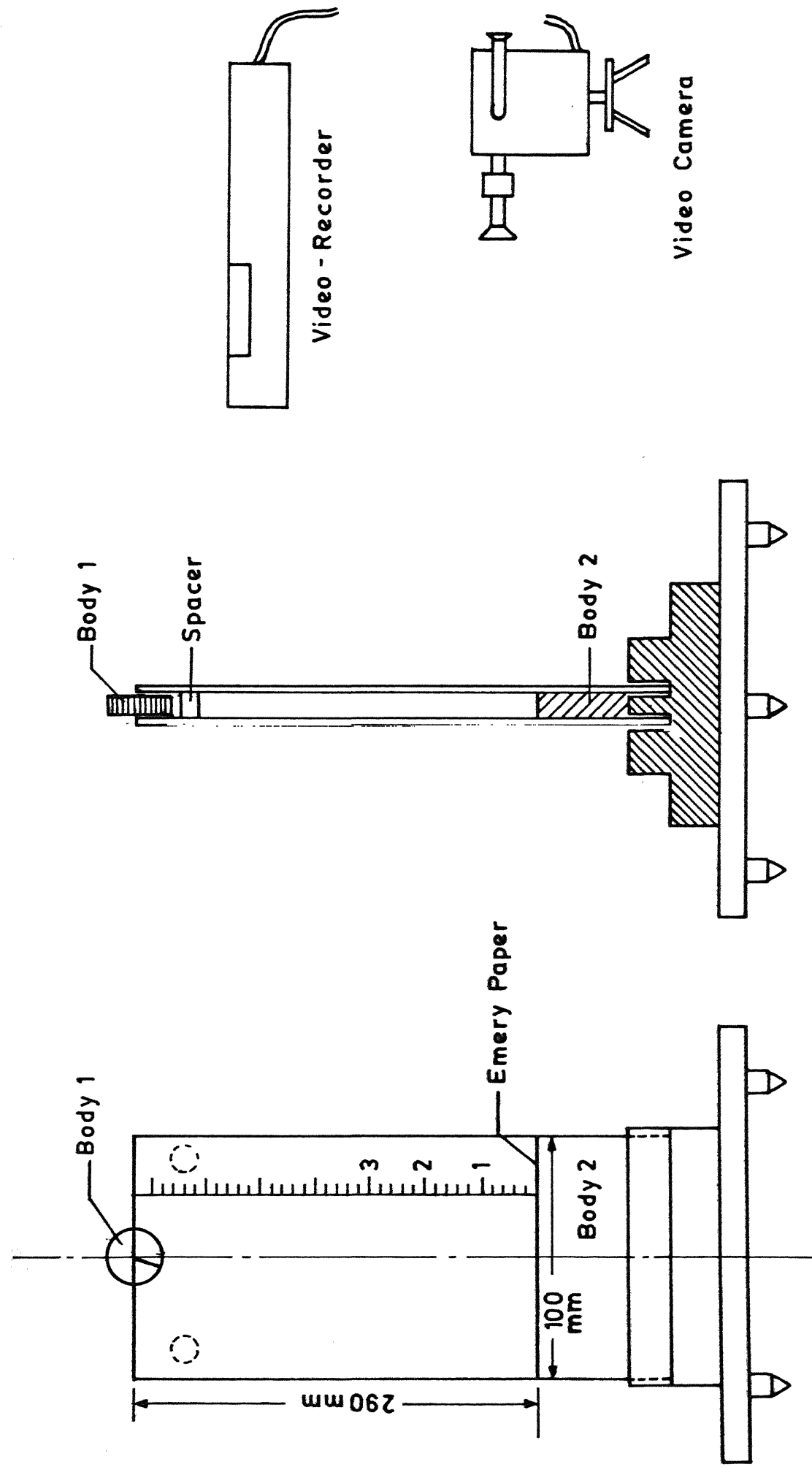


Fig. 2.6 Experimental set-up arrangement for the experiment of coefficient of restitution.

the impact. The height of bounce of body 1 is recorded by a video recorder. This experiment is repeated several times to check the repeatability of the results.

CHAPTER-3

EXPERIMENTAL RESULTS AND DISCUSSION

3.1. C.G. and M.I. of the Bodies.

Fig. 3.1 shows two bodies in a plane just at the start of impact. The centre of gravity and other dimensions are indicated in the figure. The resultant impulse of forces produced as the result of the impact is resolved into two components at the point of contact as shown in the figure. The linear velocity components of body 1 and its angular velocity about the mass centre before the impact are also indicated in the figure. The weight w_1 and moment of inertia about the mass centre, I_1 of the moving body were found out.

$$w_1 = 0.4965 \times 10^{-3} \text{ kg}$$

$$I_1 = 0.5692 \times 10^{-7} \text{ kg sec}^2 \text{m}$$

3.2 Contact Force Direction.

In fig. 3.2 are seen the photographs of fringe pattern, in order of occurrence, produced in body 2 during the process of impact. The film speed at the time of capturing the photographs was approximately 1400 frames per second and six photographs of fringe pattern could be captured. The impact produces local deformation in the bodies at the point of contact. The local deformation increases in the course of impact and is the maximum

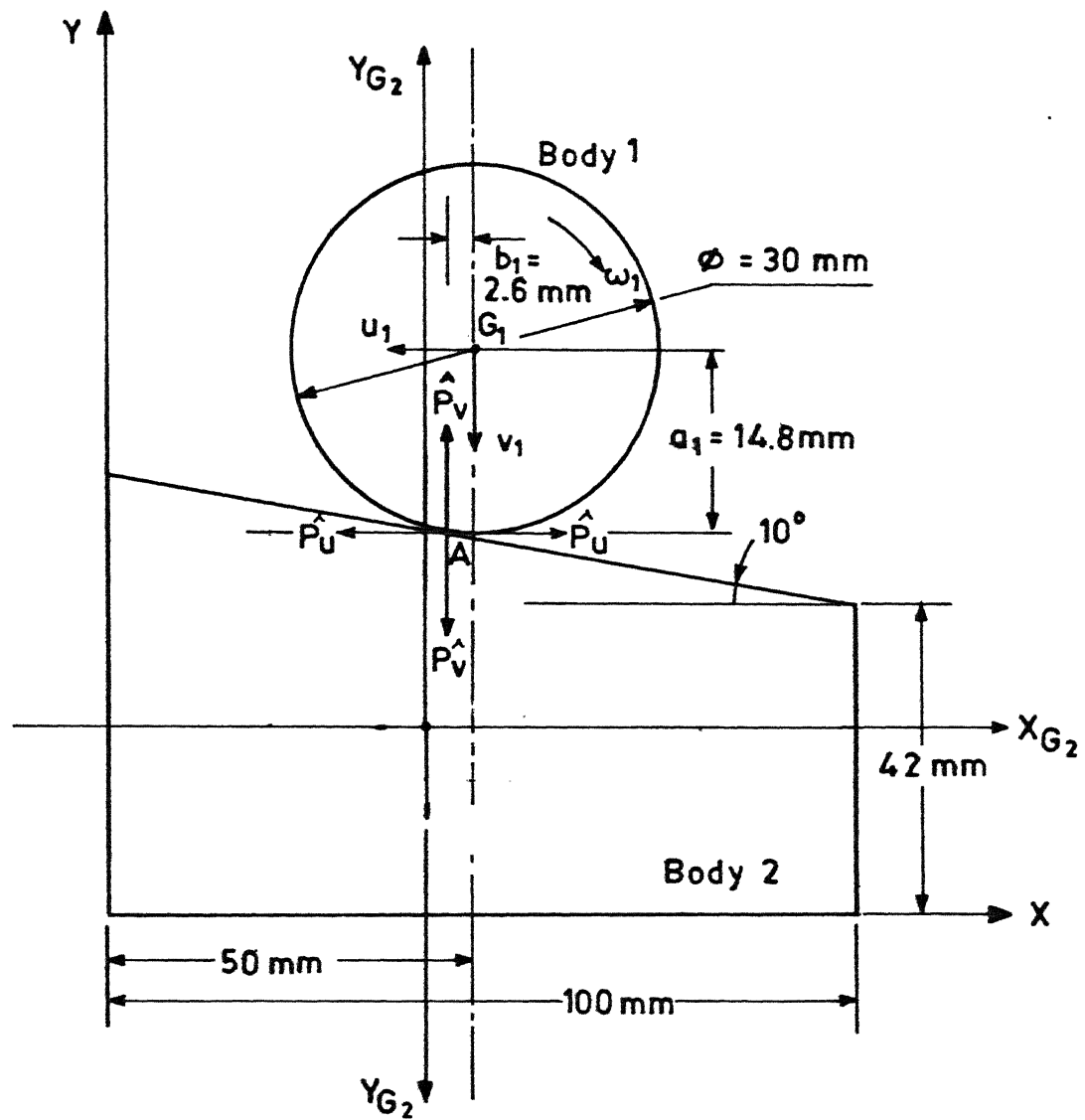


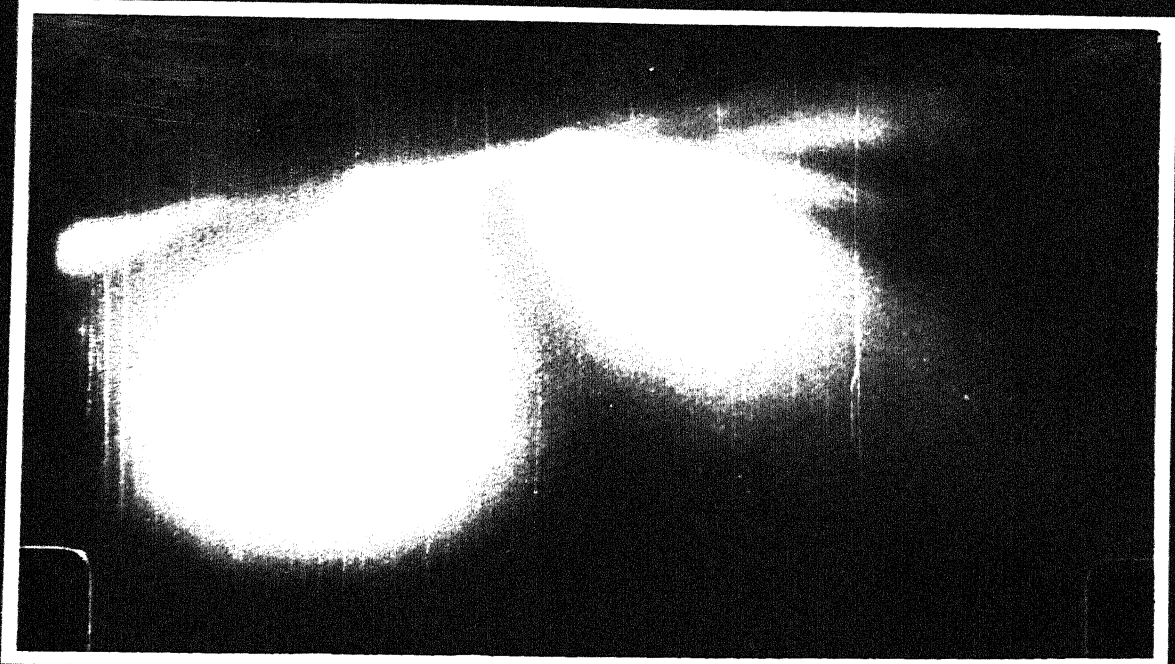
Fig. 3.1 Velocities and other dimensions of impacting bodies.

at the end of the period of approach. Looking at the photographs of the fringe pattern, it is evident that as the local deformation increases, more fringes are seen. The fringe patterns in figs. 3.2c and 3.2d indicate large deformation. The later fringe patterns in figs. 3.2e and 3.2f appertain to the period of restitution. So it is reasonable to consider that the fringe patterns in fig. 3.2a to fig. 3.2c and fig. 3.2d to fig. 3.2f are produced during the periods of approach and restitution respectively. It is found out by superimposing the fringe patterns in figs. 3.2b, 3.2c and 3.2d that axis of the two lobes of the fringe patterns does not change though the corresponding stress field in body 2 varies during the impact process. (This is illustrated in fig. 3.3). It follows that the line of action of the force produced during the periods of approach and restitution remains the same.

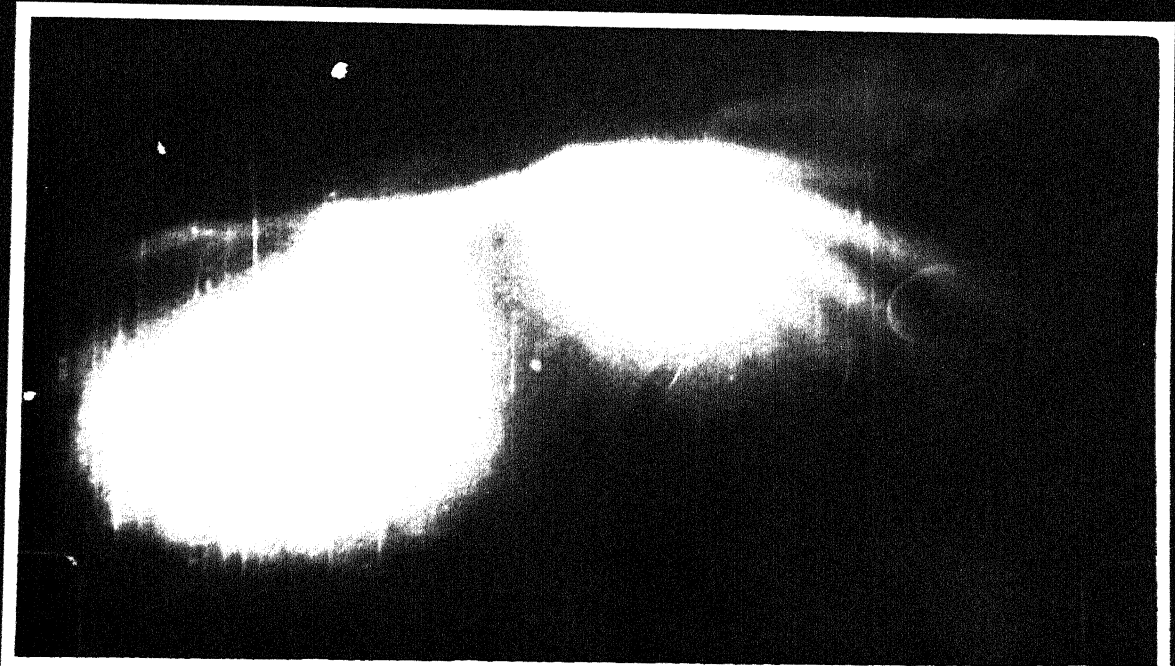
The above mentioned observation that the line of action of the forces produced as the result of the impact does not change during the periods of approach and restitution is in accordance with the assumption made by Ghosh (ref. sec. 1.2.2).

3.3.3. Velocity Measurement Results.

The photographs of positions of body 1 before and after the impact are seen in the fig. 3.4 for different trials. The photographs were captured at 64 frames per second film speed and so they show successive positions of body 1 at time intervals of



(a)

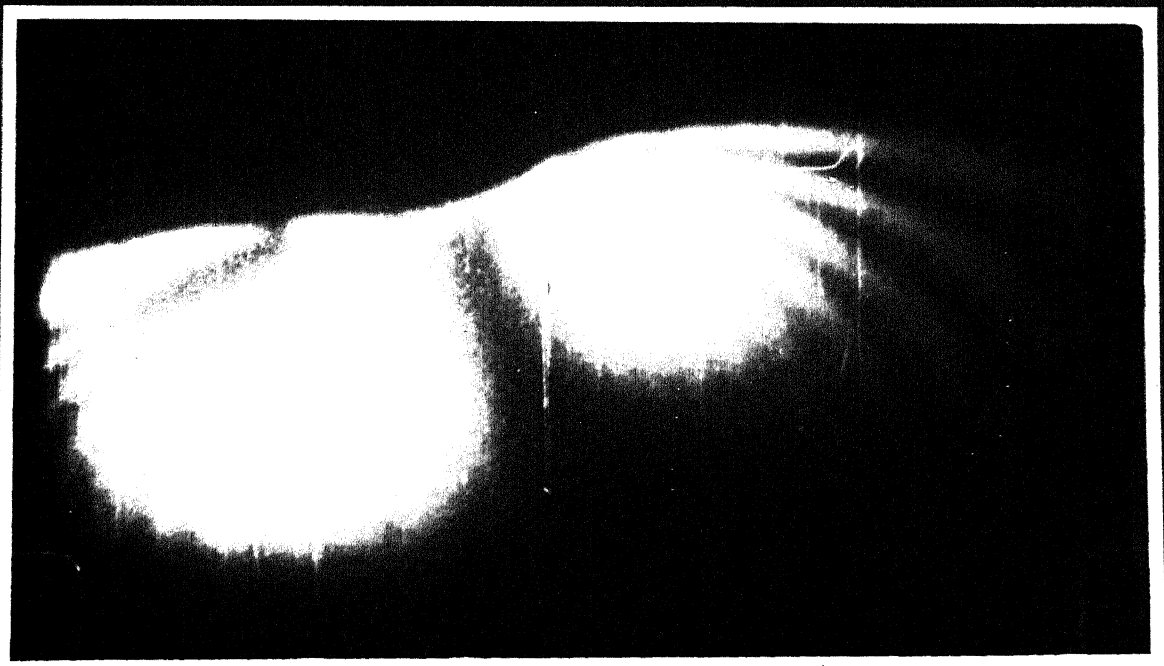


(b)

FIG. 3.2 PHOTOGRAPHS OF FRINGE PATTERN.



(c)

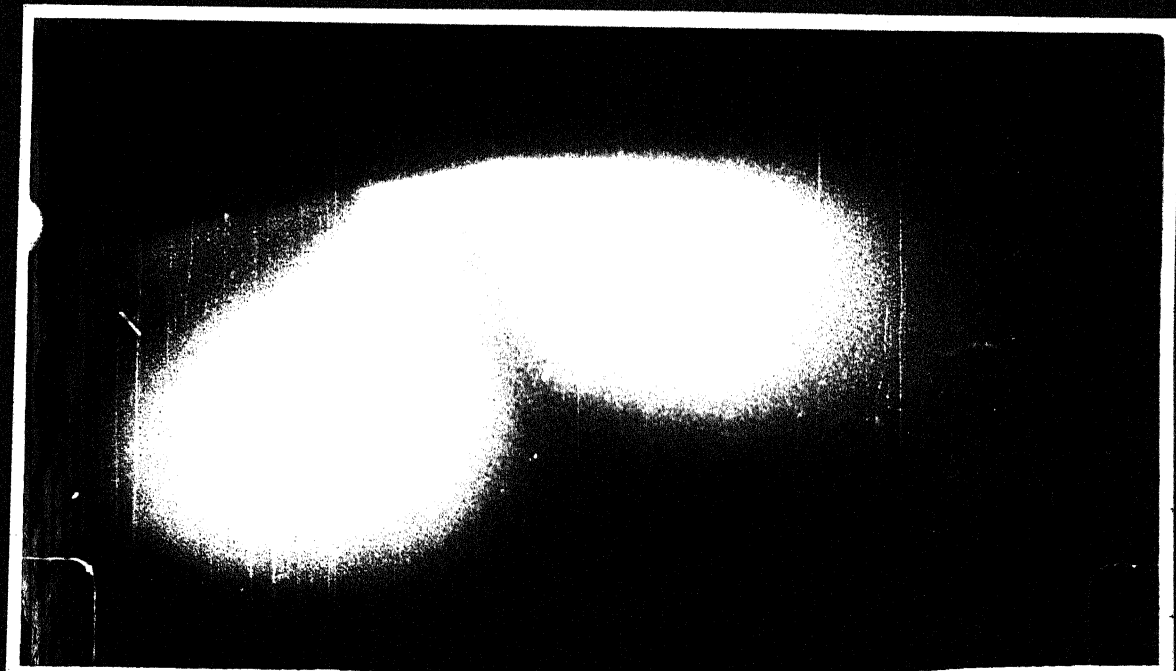


(d)

FIG. 3.2 (CONTD.)



(e)



(f)

FIG. 3.2 (CONTD.)

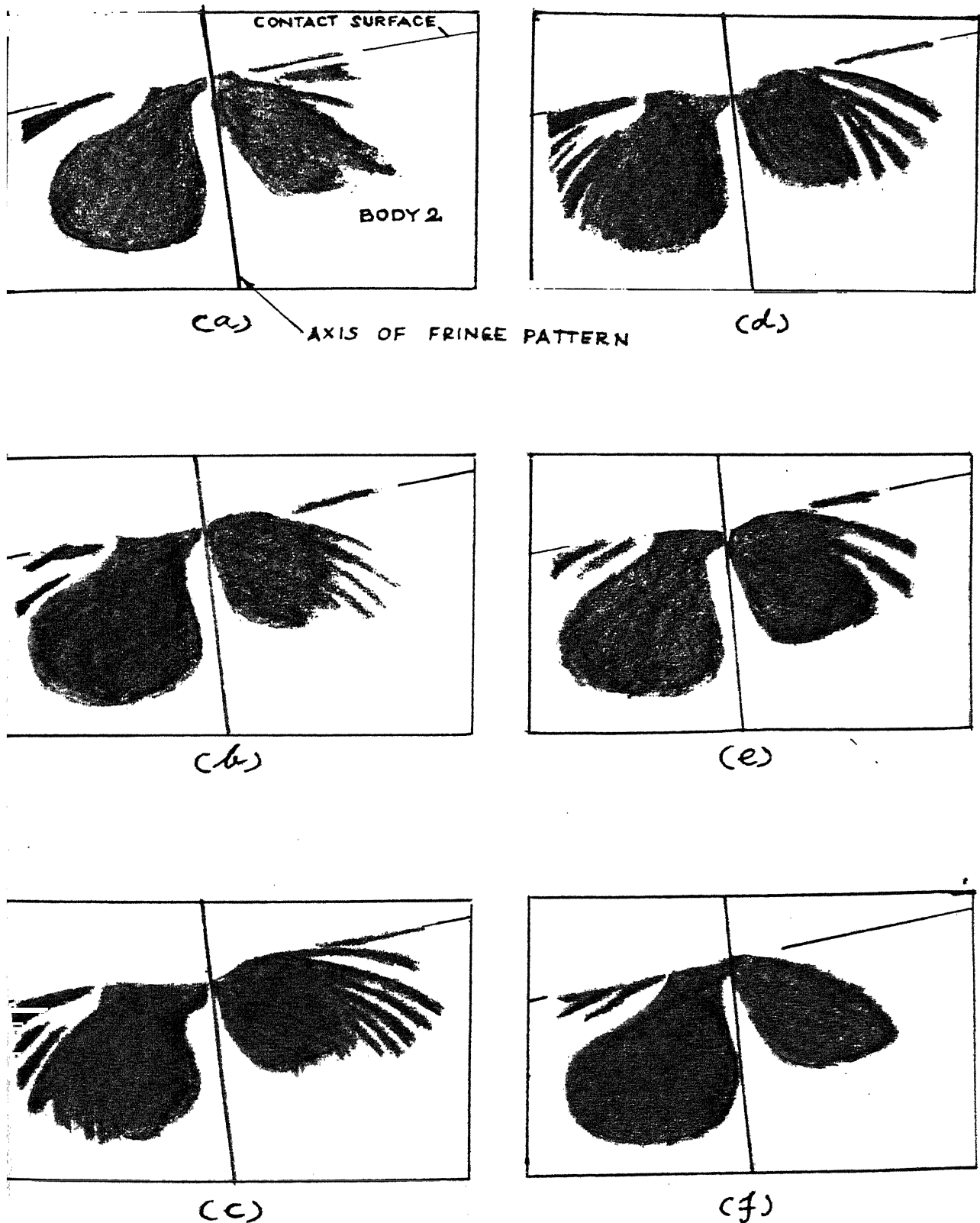


FIG. 3.3 ILLUSTRATIONS OF FRINGE PATTERNS.

1/64 second. For each trial the linear velocity components and the angular velocity about the mass centre, just before and just after the impact, are found out from the corresponding photograph as follows :

Fig. 3.5a shows schematically two successive positions of body 1 just before the impact. The body 1 is dropped freely and so only the gravitational force is acting on the body during the fall. Suppose body 1 has (x_1, y_1) and (x_2, y_2) coordinates and θ_1 and θ_2 orientation with respect to the vertical axis at position 1 and position 2 respectively, then the velocity components of body 1 in x and y directions and its angular velocity about the mass centre just before the impact can be given by following expressions :

$$u = \frac{x_2 - x_1}{t} \quad (3.1a)$$

$$v = \sqrt{v_o^2 + 2g(y_1 - y_2)} \quad (3.1b)$$

$$\omega = \frac{\theta_2 - \theta_1}{t} \quad (3.1c)$$

where v_o is the velocity of body 1 in y direction at position 1, t is the time interval between two successive photoframes (1/64 sec), u , v and ω are the velocities just before impact.

As the body 1 is dropped from the same height in all the trials,

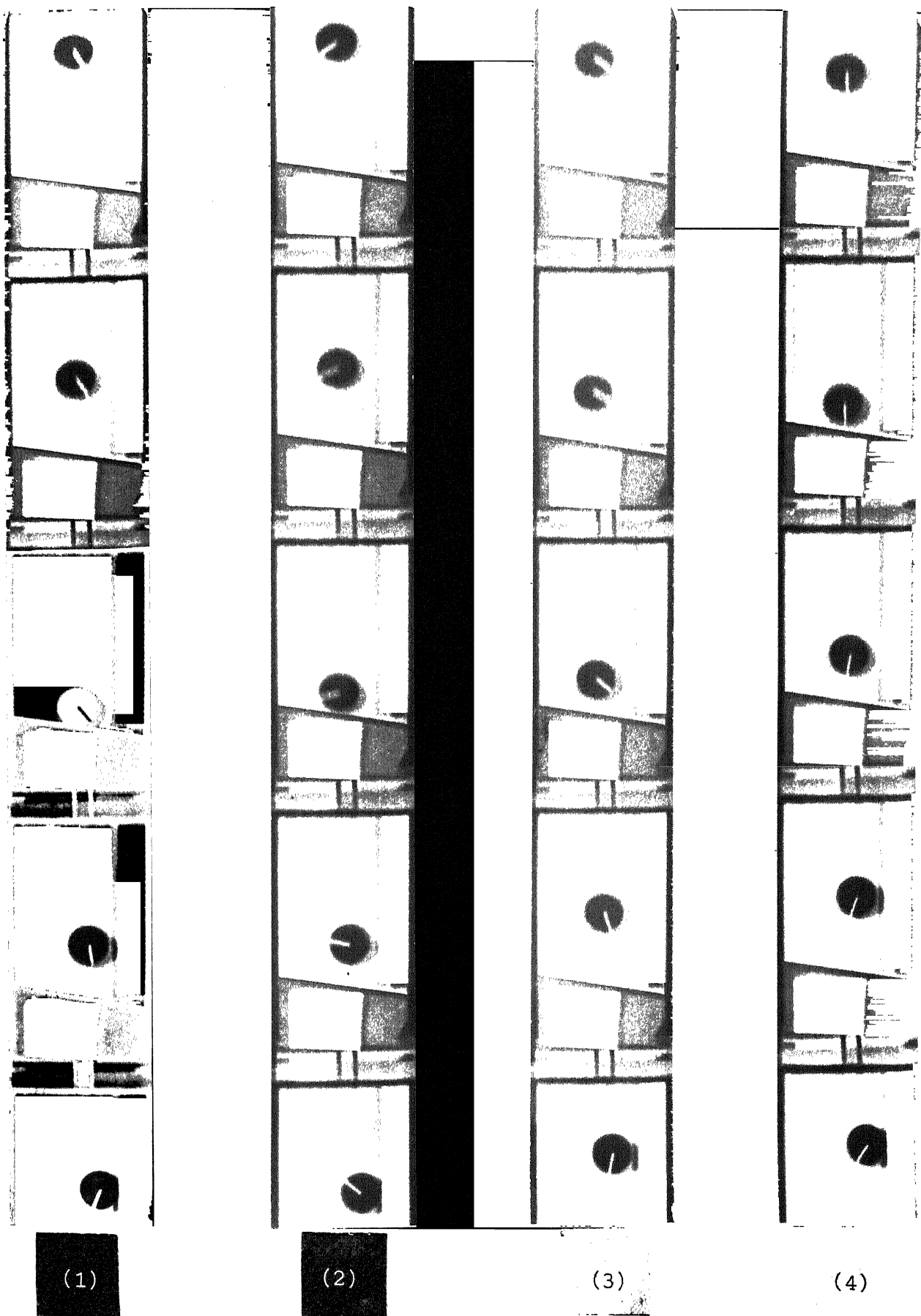


FIG. 3.4 PHOTOGRAPHS OF POSITIONS OF BODY 1 DURING IMPACT.

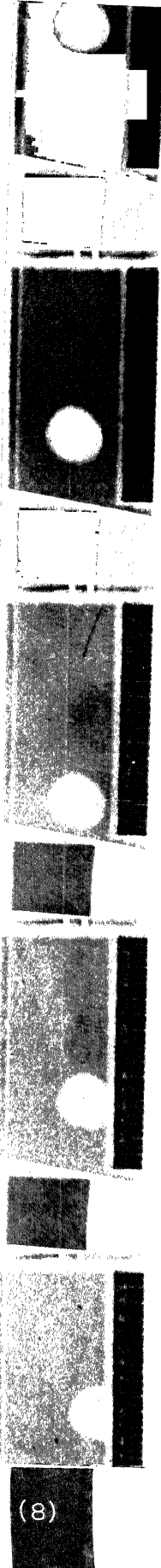
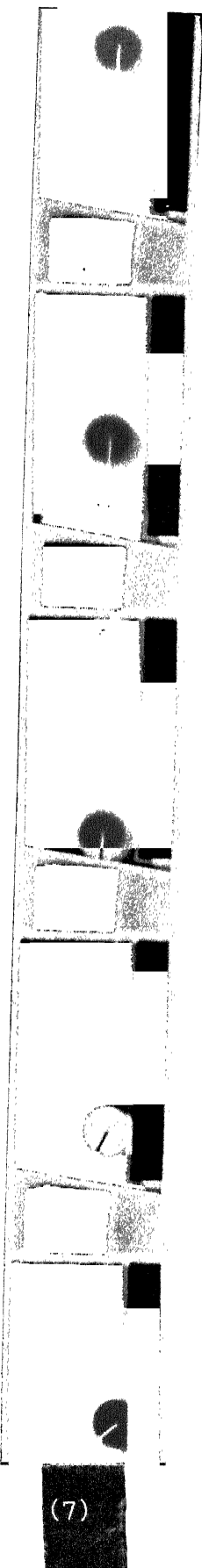
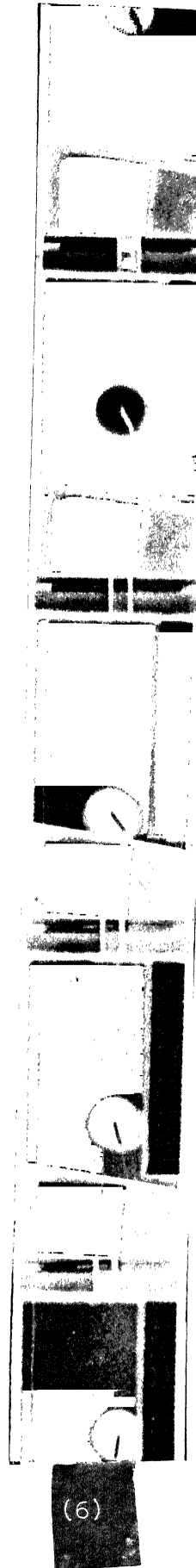
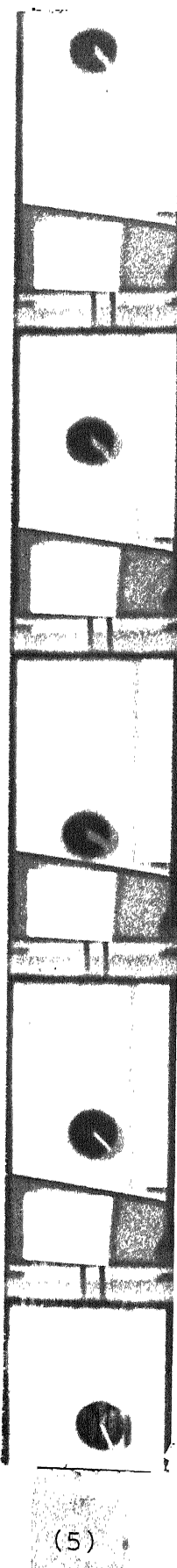


FIG. 3.4 (CONTD.)

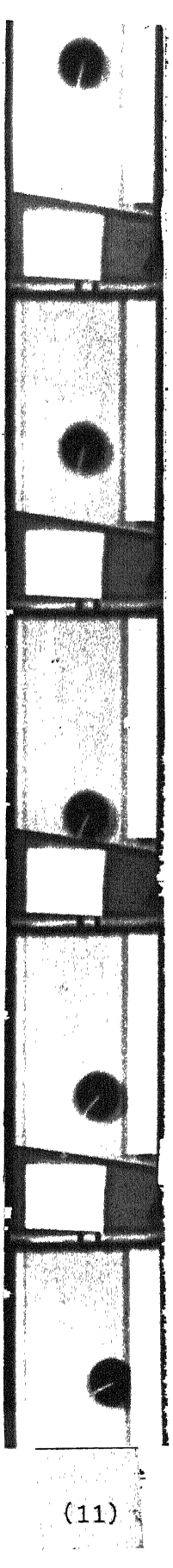
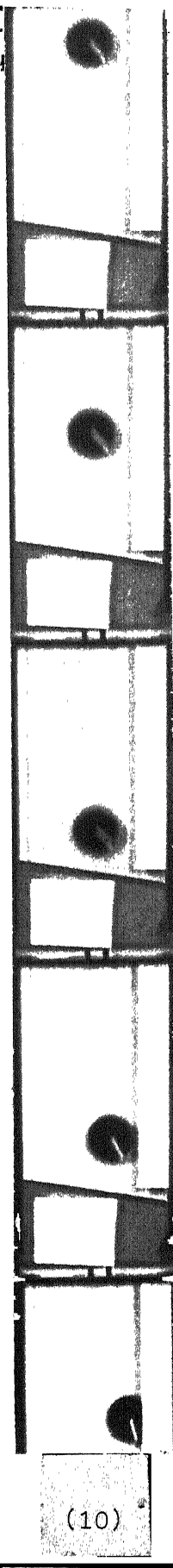


FIG. 3.4 (CONTD.)

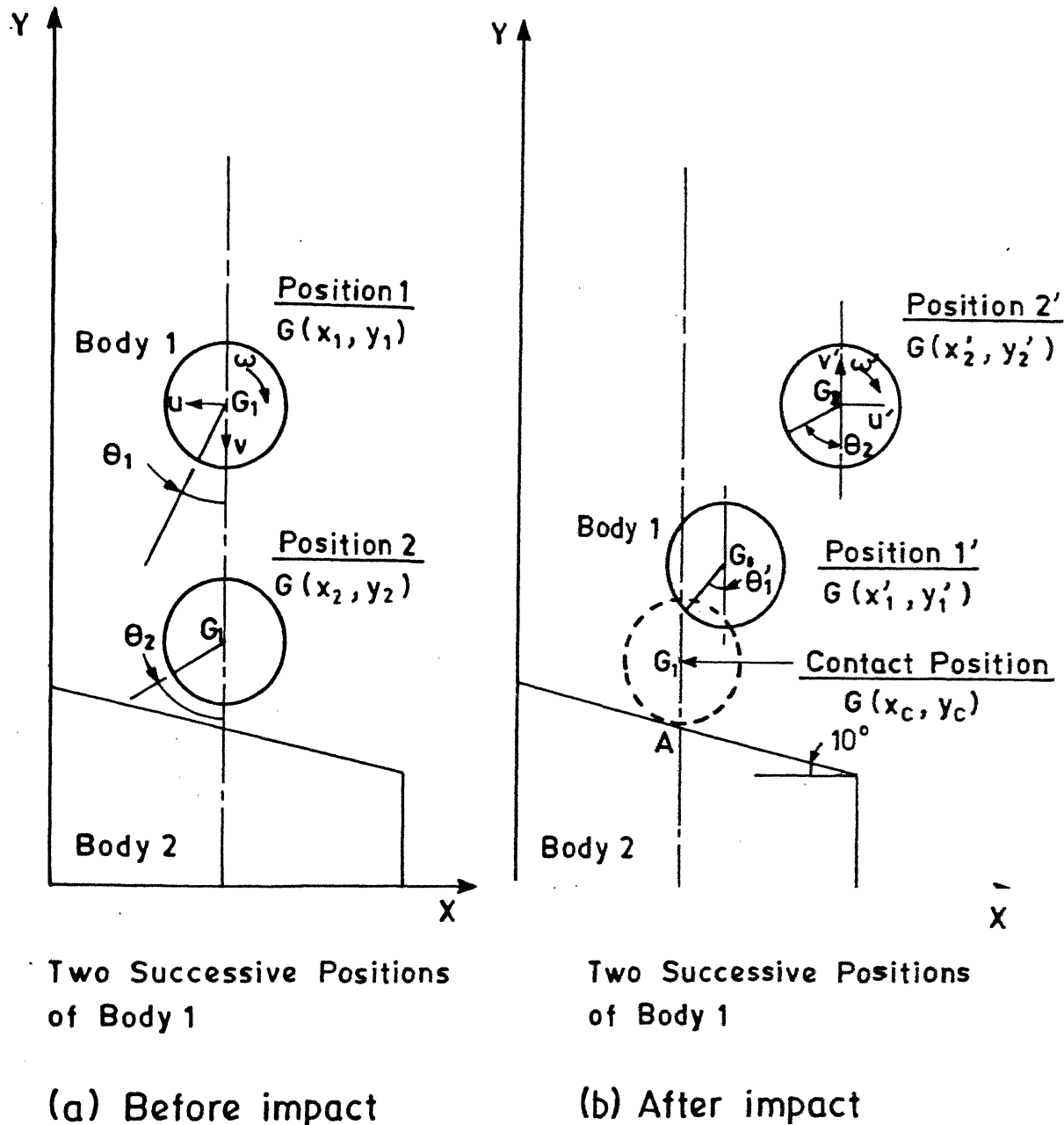


Fig. 3.5 Schematic diagram of positions of body 1 during impact.

its linear velocity in the y direction just before the impact can be given from the law of uniformly accelerated bodies as

$$v = \sqrt{2g H} \quad (3.2)$$

where H is the height of the fall ($=0.3$ m)

The results for the velocities of body 1 just before the impact are found from the above equations and are listed in Table 3.1.

Fig. 3.5b shows two successive positions of body 1 after the impact. Let the coordinates of body 1 at position 1' and position 2' be (x_1', y_1') and (x_2', y_2') and the orientation with the vertical axis be θ_1' and θ_2' respectively. Now if (x_c, y_c) be the coordinates of body 1 just at the instant of breaking contact with body 2, the velocities of body 1 just after the impact can be found out as follows :

As the body 1 is bouncing off the surface of body 2, uniform deceleration is acting on it because of the gravitational force. To determine the four unknowns (v' , u' , ω' and t_1), four equations are available as follows :

$$u' = \frac{x_2' - x_1'}{t}$$

$$u' = \frac{x_1' - x_c}{t_1}$$

$$y_1' - y_c = v' t_1 - \frac{1}{2} g t_1^2$$

$$\omega' = \frac{\theta_2' - \theta_1'}{t}$$

where t_1 is the time interval between the position 1' and the contact position, u' , v' and ω' are the velocities after the impact,

t is the time interval between the two successive photo-frames ($= \frac{1}{64}$ sec.).

Solving the above equations, we get the equations of velocities of body 1 just after the impact. They are

$$u' = \frac{x_2' - x_1'}{t} \quad (3.3a)$$

$$v' = \frac{y_1' - y_c + \frac{g}{2} [(x_1' - x_c)/(x_2' - x_1')]^2 t^2}{[(x_1' - x_c)/(x_2' - x_1')] t} \quad (3.3b)$$

$$\omega' = \frac{\theta_2' - \theta_1'}{t} \quad (3.3c)$$

The results for the velocities of body 1 just after the impact for each trial are found from the above equations and are listed in Table 3.1.

3.5 Discussion.

3.5.1. Velocities obtained using the Traditional Procedure.

The velocities of body 1 just after the impact are

TABLE 3.1 Experimentally Obtained Velocities of Body 1.

Trial Nos.	Velocities of Body 1 before Impact			Velocities of body 1 after Impact		
	u	v	ω	u'	v'	ω'
1	0	2.426	- 3.40	0.5248	1.5160	33.51
2	"	"	+14.00	0.5120	1.3659	29.05
3	"	"	0	0.4736	1.4863	14.52
4	"	"	0	0.3936	1.6012	32.95
5	"	"	- 7.82	0.5120	1.6613	22.91
6	"	"	0	0.4608	1.2004	26.80
7	"	"	0	0.5248	1.3050	28.48
8	"	"	+11.17	0.5248	0.7653	45.90
9	"	"	0	0.5824	1.2897	25.69
10	"	"	- 6.14	0.5905	1.5080	21.22
11	"	"	0	0.4992	0.6289	21.22

19
A 91930

3.4 Coefficient of Restitution (e).

The height of bounce of body 1 after the impact is recorded for different trials in a video-cassette. The height (h) is measured by connecting the video player to a TV screen (ref. fig. 3.6). In Table 3.2 are listed the results for those trials when the body 1 has only linear velocity in the y-direction before and after the impact.

The coefficient of restituation is calculated as follows :

$$\text{Coefficient of Restitution, } e = \sqrt{\frac{h}{H}}$$

where H is 290 mm and the value of h is taken from Table 3.2 as 85 mm. Substituting these values in the above equation gives

$$e = 0.54 \quad (3.4)$$

3.5 Discussion.

3.5.1 Velocities obtained using the Traditional Procedure.

The velocities of body 1 just after the impact are worked out using the traditional procedure. In this procedure, the equations relating the final and initial velocities of impacting bodies are derived considering the bodies to be perfectly rigid at the instant when impact is just over. The coefficient of restitution (e) is described as the ratio of relative departure velocity to relative approach velocity of the colliding particles along the common normal. Thus the value of e for the experiment shown in fig. 3.7 can be expressed mathematically as below.

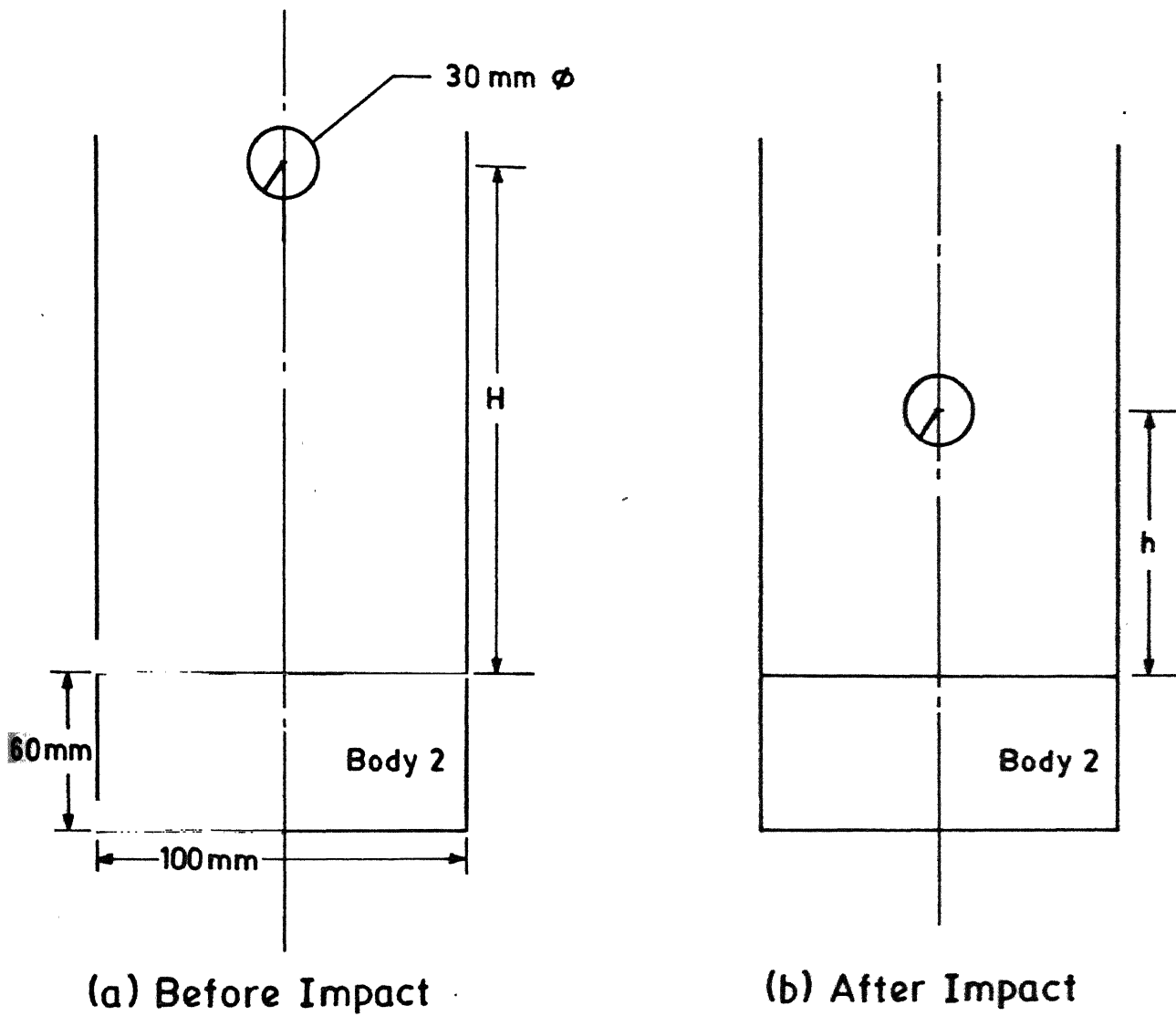


Fig. 3.6 Schematic diagram of heights of body 1 before and after impact.

TABLE 3.2 Results of h

Trial No.	Height of Bounce of Body 1, h mm	Trial No.	Height of Bounce of Body 1, h mm
1	85	17	80
2	85	18	70
3	80	19	65
4	80	20	70
5	80	21	75
6	85	22	85
7	80	23	80
8	75	24	80
9	90	25	80
10	85	26	85
11	85	27	85
12	90	28	80
13	80	29	85
14	80	30	85
15	75	31	80
16	80	32	70

$$\begin{aligned}
 e &= \frac{v_A' \text{ along the common normal}}{v_A \text{ along the common normal}} \\
 &= \frac{v' \cos \theta + u' \sin \theta}{v \cos \theta} \quad (3.5)
 \end{aligned}$$

where u' and v' are the linear velocity components of body 1 after the impact, v is the velocity of body 1 before the impact.

To determine the three unknown velocities (u' , v' and ω') of body 1 just after the impact, the required three equations

- (i) One equation is obtained from the law of inelastic impact as given in eq. 3.5.
- (ii) One equation is obtained considering the no slip condition at the point of contact.

$$r \omega' = v' \sin \theta - u' \cos \theta$$

- (iii) Conservation of the total angular momentum of the system about the contact point A gives the required third equation i.e.,

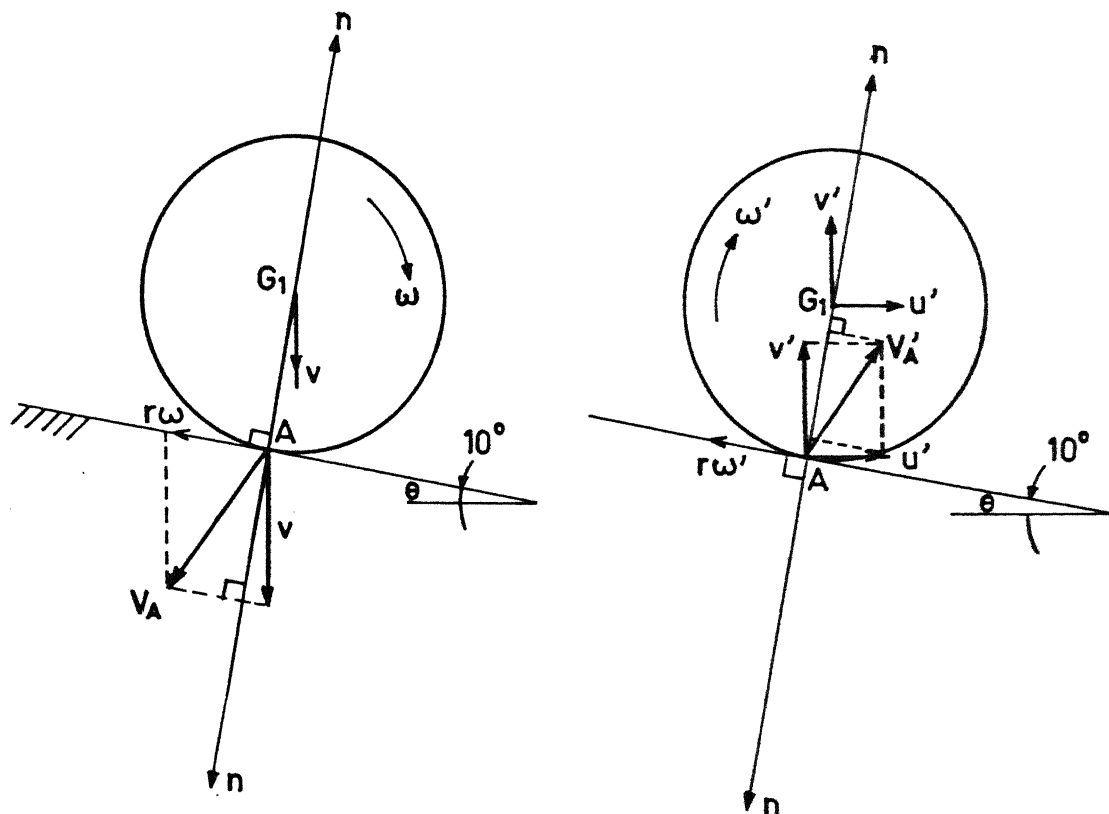
$$I \omega + mv r \sin \theta = I \omega' + mu' r \cos \theta - mv' r \sin \theta$$

Solving the above three equations, the expressions for the velocities of body 1 just after the impact are obtained as follows :

$$u' = v \cos \theta \sin \theta (e + \frac{2}{3}) + \frac{1}{3} r \cos \theta \omega \quad (3.6a)$$

$$v' = (e \cos^2 \theta - \frac{2}{3} \sin^2 \theta)v - \frac{1}{3} r \sin \theta \omega \quad (3.6b)$$

nn — Common normal to the contacting surfaces
 V_A, V'_A — Approach and departure velocity of contacting particle A respectively.



$$V_A \text{ along the common normal} \\ = v \cos \theta$$

(a) Before impact

$$V'_A \text{ along the common normal} \\ = v' \cos \theta + u' \sin \theta$$

(b) After impact

Fig. 3.7 Determination of coefficient of restitution using Traditional procedure.

$$\omega' = \frac{2v \sin \theta + r\omega}{3r} \quad (3.6c)$$

The theoretical values of velocities of body 1 just after the impact are found out from above equations by putting the initial velocities of body 1 from Table 3.1 and value of coefficient of restitution from eq. 3.4. The results are listed in Table 3.3.

3.5.2. Velocities obtained using the Proposed Procedure.

The velocities of body 1 just after the impact have also been determined using the proposed procedure as mentioned in sec. 1.2.2. In this procedure, the equations relating the final and initial velocities of body 1 are found by considering the two bodies to be perfectly rigid at the threshold of the periods of approach and restitution. The coefficient of restitution (e) is described as the ratio of the relative total departure velocity to the relative total approach velocity of the colliding particles (ref. fig. 3.8). The value of e in the experiment can be expressed mathematically as below.

$$e = \frac{\frac{V_A'}{V_A}}{= \frac{\sqrt{(v' + r\omega' \sin \theta)^2 + (r\omega' \cos \theta - u')^2}}{\sqrt{(v - r\omega \sin \theta)^2 + (r\omega \cos \theta)^2}}} \quad (3.7)$$

To determine the three unknown velocities (u' , v' , and ω') of body 1 just after the impact, the required three equations

TABLE 3.3 Results Obtained Using Traditional Procedure

Trial No.	Angular velocity before impact (rad/sec)	Theoretical Velocity Results (after impact)		
		u' (m/sec)	v' (m/sec)	ω' (rad/sec)
1	-3.4	0.4839	1.2248	17.59
2	+14.0	0.5695	1.2097	23.38
3	0	0.5006	1.2218	18.72
4	0	0.5006	1.2218	18.72
5	-7.82	0.4621	1.2286	16.11
6	0	0.5006	1.2218	18.72
7	0	0.5006	1.2218	18.72
8	+11.17	0.5556	1.2121	22.44
9	0	0.5006	1.2218	18.72
10	-6.14	0.4704	1.2271	16.67
11	0	0.5006	1.2218	18.72

are obtained as follows :

(i) One equation is obtained by conserving the total angular momentum of the system about the contact point A; i.e.,

$$I \omega + mv r \sin \theta = I \omega' + mu' r \cos \theta - mv' r \sin \theta \quad (3.8)$$

(ii) Two equations are obtained from the consideration that the direction of the impulse of forces acting during the periods of approach and restitution remains same. Then the law of inelastic impact implies that the energy loss factors in both the normal and shear directions are same, i.e.

$$u_A' = e u_A \quad (3.9a)$$

$$v_A' = e v_A \quad (3.9b)$$

where u_A , v_A and u_A' , v_A' are the components of linear velocities of contacting particle A before and after the impact respectively. The above condition (eqs. 3.9) gives two equations as below.

$$v' + r \omega' \sin \theta = e(v - r \omega \sin \theta) \quad (3.10a)$$

$$u' - r \omega' \cos \theta = e r \omega \cos \theta \quad (3.10b)$$

Solving the eqs. 3.8, 3.10a and 3.10b, velocities of body 1 just after the impact are obtained in terms of its initial velocities as below.

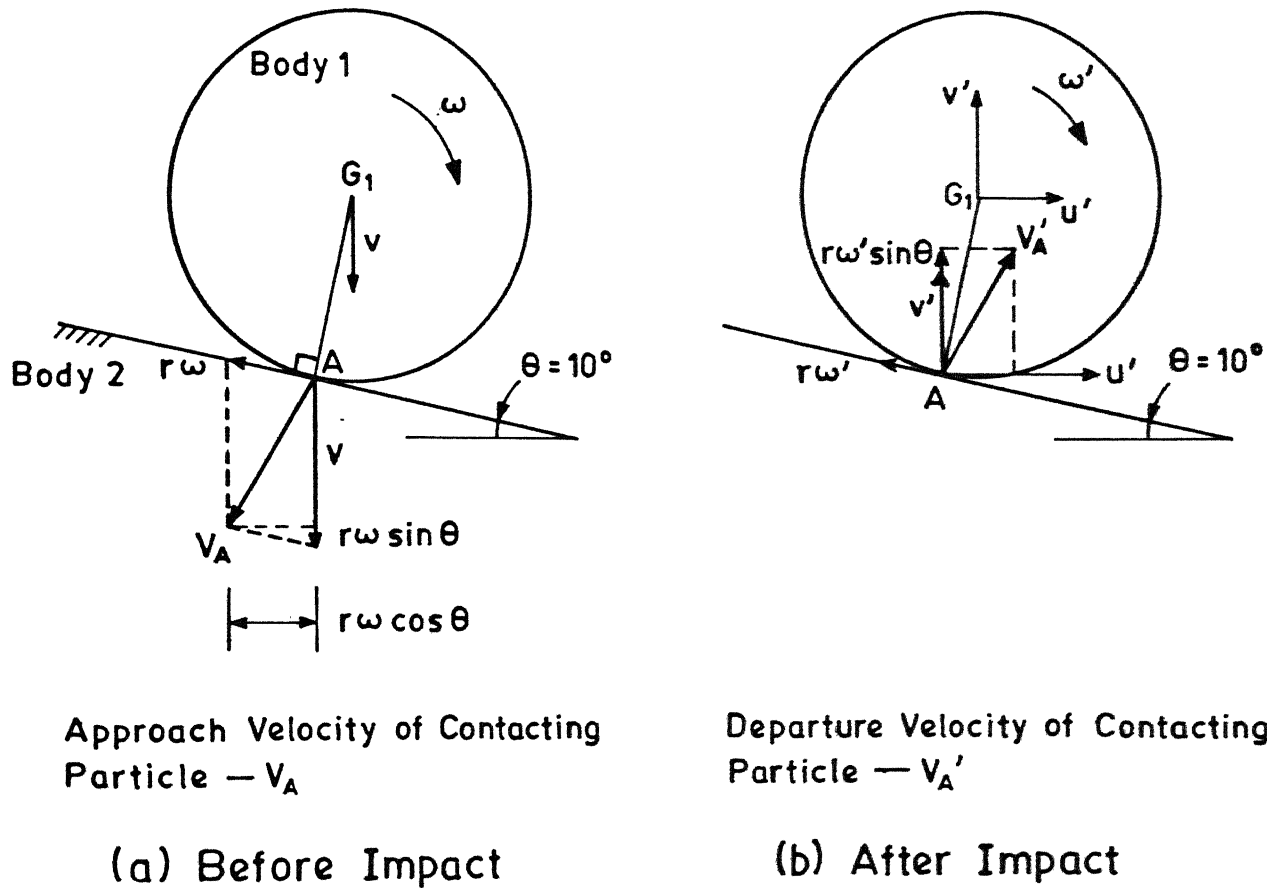


Fig. 3.8 Determination of coefficient of restitution using proposed procedure.

$$u' = \frac{2}{3} \cos \theta \sin \theta (1 + e) v + \frac{1}{3} r \omega \cos \theta (1 + e) \quad (3.11a)$$

$$v' = [e - \frac{2}{3} \sin^2 \theta (1 + e)] v - \frac{1}{3} r \omega \sin \theta (1 + e) \quad (3.11b)$$

$$\omega' = [\frac{2}{3} \frac{\sin \theta (1+e) v + r\omega (\frac{1}{2} - e)}{r}] \quad (3.11c)$$

The theoretical values of velocities of body 1 just after the impact for each trial are worked out by putting the initial velocities of body 1 from Table 3.1 and value of e from eq. 3.4; these results are listed in Table 3.4.

Now the average velocity components and the average angular velocity after the impact were calculated from the experimental results (Table 3.1) for the trials in which angular velocity before impact are zero. To make the comparative analysis of the velocity results obtained from the traditional procedure and the proposed procedure, the results for velocities after the impact for $\omega = 0$ are listed in Table 3.5.

It is seen from Table 3.5 that the result for the angular velocity after impact (ω'), obtained from the proposed procedure, is slightly closer to the average experimental value (ω'). The comparison of the linear velocity components shows that the difference in the results for the linear velocity component in the y direction (v') obtained from the traditional and proposed procedure is insignificant. However, the results for the linear velocity components in the x direction (u') reveals that

TABLE 3.4 Results Obtained Using Proposed Procedure

Trial No.	Angular velocity before impact (rad/sec)	Theoretical Velocity Results (after impact)		
		u' (m/sec)	v' (m/sec)	ω' (rad/sec)
1	-3.4	0.4001	1.2395	28.92
2	+14.0	0.5320	1.2162	28.46
3	0	0.4259	1.2349	28.83
4	0	0.4259	1.2349	28.83
5	-7.82	0.3660	1.2454	29.04
6	0	0.4259	1.2349	28.83
7	0	0.4259	1.2349	28.83
8	+11.17	0.5106	1.2200	28.53
9	0	0.4259	1.2349	28.83
10	-6.14	0.3793	1.2431	28.99
11	0	0.4259	1.2349	28.83

TABLE 3.5 Velocity Results (for initial $\omega = 0$).

Velocities after impact	Experimental Results (average value)	Theoretical Results	
		Traditional Procedure	Proposed Procedure
u' (m/sec)	0.4880	0.5006	0.4259
v' (m./sec)	1.2519	1.2248	1.2349
ω' (rad/sec)	24.94	18.72	28.83

the value of u' obtained from the proposed procedure is smaller than the average experimental value for u' , while the value of u' obtained from the traditional procedure is larger. The reason for the discrepancy in the results for the velocities after the impact, obtained from the proposed procedure and the experiments, can possibly be attributed to the slip occurring at the contact point.

CHAPTER-4

CONCLUSIONS

In the experiment of determination of the contact force direction, it is found from the photographs of fringe pattern that the line of action of forces produced as the result of the impact does not change during the impact interval. The above observation follows that the coefficient of restitution in the normal and shear directions remains same. So it is correct to determine the coefficient of resitution as mentioned in sec.

1.2.2.

The results for the velocities of the moving body just after the impact obtained from the traditional procedure and the proposed procedure are not significantly different compared to the average experimental results. However, the results for the angular velocity after the impact, obtained from the proposed procedure, are marginally closer to the experimental values.

REFERENCES

1. McMillan, W.D., "Dynamics of Rigid Bodies", McGraw-Hill Book Co. Inc., 1935, p. 332.
2. Whittaker, E.T., "A Treatise on the Analytical Dynamics of Particles and Rigid Bodies", Cambridge Univ. Press, 1961, p. 238.
3. Smart, E.H., "Advanced Dynamics, Vol. II", McMillan & Co. Ltd., London, 1951, p. 148.
4. Loney, S.L., "An Elementary Treatise on the Dynamics of a Particle and of Rigid Bodies", Cambridge Univ. Press, 1960, p. 264.
5. Goldsmith, W., "Impact - The Theory and Physical Behaviour of Colliding Solids", Edward Arnold Ltd., London, 1960.
6. Dally, J.W. and Riley, W.F., "Experimental Stress Analysis", McGraw-Hill Book Co. Inc., 1978, Ch. 3.

A 91930

ME-1586-M-SHA-EXP